

AD 690189

CLOUD CHEMISTRY OF FALLOUT FORMATION FINAL REPORT
OCK Work No. 3111A T.O. No. 3110(68) GGA

Gulf General Atomic
Incorporated

GA-9180

OCD Work No. 3111A T.O. No. 3110(68)

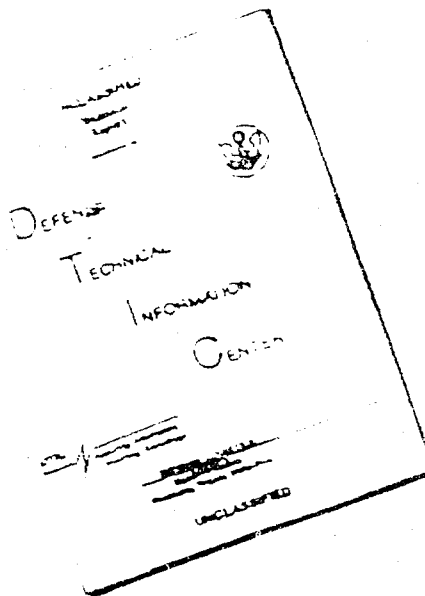
**CLOUD CHEMISTRY OF FALLOUT FORMATION
FINAL REPORT**

This document has been approved for public
release and sale; its distribution is unlimited.

January 31, 1969

JUN 19 1969
RECEIVED
G-2

DISCLAIMER NOTICE



THIS DOCUMENT IS BEST
QUALITY AVAILABLE. THE COPY
FURNISHED TO DTIC CONTAINED
A SIGNIFICANT NUMBER OF
PAGES WHICH DO NOT
REPRODUCE LEGIBLY.

REPRODUCED FROM
BEST AVAILABLE COPY

Gulf General Atomic
Incorporated

P O Box 608, San Diego, California 92112

GA-9180

CCD Work No. 3111A T.O. No. 3110(68)

CLOUD CHEMISTRY OF FALLOUT FORMATION
FINAL REPORT

by

J. H. Norman, P. Winchell,
and H. G. Staley

for

Office of Civil Defense
Office of the Secretary of the Army
Washington, D.C. 20310

under

Contract N0022868C2376

OCD REVIEW NOTICE

This report has been reviewed in the Office of Civil Defense and approved for publication. Approval does not signify that the contents necessarily reflect the views and policies of the Office of Civil Defense.

This document has been approved for public release and sale; its distribution is unlimited.

Gulf General Atomic Project 6063

January 31, 1969

CLOUD CHEMISTRY OF FALLOUT FORMATION
FINAL REPORT

by

J. H. Norman, P. Winchell, and H. G. Staley
Gulf General Atomic Incorporated Report GA-9180
January 31, 1969

SUMMARY

Studies of fission-product gamma emanation shortly after fission (1 to 100 sec) have been initiated. The half-lives that will be established in this program, when used in conjunction with initial yields, will provide the fission-product yield history for calculational models. The studies undertaken include (1) an investigation of the transitive behavior of fission products from approximately 1 sec after fission, (2) experiments to establish recoil range as a parameter to use for identifying the sources of specific gamma rays, and (3) design of a steady-state tape system for catching and subsequently investigating recoil-fission products. This latter study is the result of earlier investigations and shows promise of providing extensive, accurate data on fission-product half-lives.

Studies of diffusion of various nuclides in the $\text{CaO-Al}_2\text{O}_3\text{-SiO}_2$ system, the $\text{Na}_2\text{O-Al}_2\text{O}_3\text{-SiO}_2$ system, and Small Boy soil from the Nevada test site have been made. The use of fission products from slow U-235 fission in situ has been demonstrated as a surveying method for studying diffusion in various matrices doped with U-235. The results of the studies are consistent with the compensation law, particularly with the compensated data developed previously in this program. The liquid-structure factor appears to be important in establishing diffusivities.

Transpiration studies of the volatility of Cs from $\text{CaO-Al}_2\text{O}_3\text{-SiO}_2$ solutions indicate that simple gas-phase transport laws apply to transpired Cs. The condensed-state and vapor-state chemistry of this system have not been totally resolved.

A mathematical description of sorption of gaseous components by a particle, using condensation coefficients and condensed-state diffusion coefficients, is presented. This treatment suggests that condensation coefficients become important to the process when they are lower than approximately 2×10^{-6} .

Mass spectrometric studies have been made that provide estimates of the stabilities of the gaseous species Sb_4O_6 , As_4O_6 , SbO , TeO , and TeO_2 . The gaseous species AsO_2 and SbO_2 were not observed, thus their stabilities could not be measured.

CONTENTS

INTRODUCTION	1
SHORT-LIVED FISSION-PRODUCT STUDIES.....	2
Initial Transient Studies	2
Recoil-Range Studies	4
Steady-State Short-Lived Fission-Product Studies	15
Unfolding Gamma-Ray Spectra	20
DIFFUSION OF RADIONUCLIDES IN MOLTEN SILICATES	23
Diffusion in the $\text{Na}_2\text{O}-\text{Al}_2\text{O}_3-\text{SiO}_2$ System	23
Diffusion in Molten Nevada Soil.....	31
Diffusion in the $\text{CaO}-\text{Al}_2\text{O}_3-\text{SiO}_2$ System	34
Compensation Law	38
HENRY'S LAW CONSTANT MEASUREMENTS.....	41
THE ROLE OF CONDENSATION COEFFICIENTS IN FALLOUT FORMATION	43
MASS SPECTROMETRY OF OXIDE SYSTEMS	47
PUBLICATIONS AND PRESENTATIONS	52
REFERENCES	53

FIGURES

1. Fission-product mass vs. recoil parameter	5
2. Spectrum for second film taken 26 to 66 min after fission (1-hr irradiation).....	7
3. Recoil-range parameters at various times for the observed spectral lines of I-135	18

FIGURES (continued)

4.	Fission-product recoil-range parameter C_3/C_2 in Mylar vs. atomic mass	19
5.	Steady-state recoil fission-product experiment	21
6.	Phase diagram for the sodium disilicate-albite system showing parameters of diffusion experiments	25
7.	Diffusion coefficients for the transport of Sb-124 in liquids from the sodium disilicate-albite system as a function of temperature	28
8.	Comparison of energies of activation for diffusion in molten media with the sodium disilicate-albite phase diagram	30
9.	Diffusion coefficients for transport of Sb-124 in vitreous and devitrified Nevada soil as a function of temperature	33
10.	Compensation correlation for the transport of fission-product species in Matrix B.	37
11.	Compensation correlation for data obtained at GGA for diffusion in silicates. Solid circles refer to data obtained this contract year	39
12.	A typical temperature dependence of the equilibrium constant of Reaction 27 for As	48
13.	A typical temperature dependence of the equilibrium constant of Reaction 27 for Sb.	49

TABLES

1.	Energies of Recovered Gamma Rays	3
2.	Fission-Product Gamma-Energy/Recoil-Range Correlation. . .	16
3.	Diffusivities for Transport of Na-24 in Melts from Sodium Disilicate-Albite System	24
4.	Arrhenius Parameters for Diffusion of Na-24 in Melts from the Sodium Disilicate-Albite System	26
5.	Experimental and Predicted Arrhenius Parameters for Diffusion in Melts of Albite Composition	27
6.	Diffusion Coefficients for the Transport of Radioantimony in Liquids from the Sodium Disilicate-Albite System	29

TABLES (continued)

7.	Arrhenius Parameters for Sb-124 Diffusion in Melts from the Sodium Disilicate-Albite System	29
8.	Diffusion Coefficients for the Transport of Radioantimony in the Nevada Matrix.	32
9.	Diffusion Coefficients for Transport of Fission-Product Nuclides in Matrix A at 1773°K.	35
10.	Diffusion Coefficients for Transport of Fission-Product Nuclides in Matrix B.	36
11.	Coefficients in the Diffusion Equation for Transport in Matrix B	38
12.	Summary of the Heats and Entropies for Reaction 27	50
13.	Results of the Pressure Calibration and Calculated Entropy for Reaction 28	51

INTRODUCTION

In the past, fallout studies at Gulf General Atomic have been concerned with evaluating chemical fractionation of fission products during fallout formation. The studies presented in this report are an integral part of this evaluation, but the area to be studied has been somewhat changed. Henry's law studies are not, as in former studies, the only major concern of the work presented here. In place of Henry's law studies, more effort has been spent on the delineation of the history of isotopic species present in the cloud. This is manifest in a program to determine half-lives of early fission-product nuclides. Although only preliminary studies have been made the results are very promising and it is anticipated that considerable knowledge can be obtained concerning fission-product half-lives in the time region of 1 to 100 sec after fission.

More concern is being given the condensation process in fallout formation. Calculational studies of controlling factors for sorption of fission products by fallout have been made. A range of importance of condensation coefficients is suggested herein, and experimental measurements have been proposed.

The diffusion studies program is considered to be so important that it has been expanded. More work on surveying methods and theoretical studies is presented. Studies of various matrices are important, and the matrix problem is of major concern in supplying data for a diffusion-controlled fission-product sorption model.

Thermodynamic studies of various gaseous systems have been continued. These mass spectrometric studies are valuable in that they provide the basic data required for estimating Henry's law constants.

SHORT-LIVED FISSION-PRODUCT STUDIES

As a part of this study an investigation of fission-product gamma spectra shortly after fission, as a function of time after fission, has been initiated. The purpose of this study is to delineate half-lives of some of the fission products that have not yet been studied in detail. This information is important to a model describing fallout formation because the chemical properties and abundances of the isotopes during fallout formation define the fractionation of fission products in fallout. Given initial fission-product yields, fission-product half-lives are used to define the quantities of each isotope present after detonation.

INITIAL TRANSIENT STUDIES

Half-life studies may be performed in several ways. A first investigation using a pulsing TRIGA reactor and a "rabbit" tube has been made. The rabbit tube is a pneumatic tube in which a sample can be rapidly delivered to the spectrometer-detector system from the reactor. The detector system consists of a 4096-channel analyzer and appropriate computational equipment. The pulsing-reactor/rabbit-tube system had been previously set up at the TRIGA facility.

In this experiment, 1 mg of natural U in 0.2 g of pure C was subjected to approximately 2×10^{14} thermal neutrons/cm³ in approximately 0.02 sec, causing about 2×10^9 fissions. This sample was rabbitied to a position about one foot from a 3 cm³ Ge-Li detector and counted from the time of arrival (approximately 0.6 sec after pulsing) until 2 sec after pulsing. It was recounted during succeeding 6-sec intervals or multiples thereof for about 18 min, shortening the sample detector distance when appropriate. The resulting spectra were subjected to a computer search program to identify the various gamma rays according to energy and to evaluate their intensity. Table 1 is a listing of energies of gamma rays recovered by the programs during this study. To be included in this table, a peak must have been recovered from at least three consecutive spectra.

None of these peaks have been identified so far. However, gamma rays from Cs-138 were observed in the last two spectra. Some other peaks have energies corresponding to reported values from certain fission products, but the effort afforded to this work so far has led to few identifications. This identification problem was previously recognized by Gordon, Harvey, and Nakahara. (1)

TABLE 1
ENERGIES OF RECOVERED GAMMA RAYS

Energy (KeV)	No. of Spectra Including This Peak	Time of First Recovery (sec)
85	18	0.6
104	7	31
111	7	258.5
127	5	381.5
132	10	0.6
146	10	2.5
160	11	101
169	4	0.6
178	6	320
200	10	101
206	6	2.5
227	15	2.5
239	10	75.5
266	8	209
292	4	320
310	6	46
318	11	101
349	7	132.5
403	6	10
412	10	75.5
438	7	258.5
458	7	75.5
464	5	381.5
544	7	2.5
590	13	31
642	7	132.5
658	3	664.5
721	8	164
789	4	443
830	5	31
912	6	258.5
968	9	2.5
1195	6	207.5
1236	7	207.5

One of the major problems with the 4096-channel-analyzed data is the long signal-processing time (approximately 100 microseconds). This means that a maximum of only 10,000 pulses/sec can be received, which is a weak signal when divided into the individual gamma peaks. More extensive data will be required for accurate studies, presumably from steady-state system studies. In addition to providing more accuracy on the presently recovered peaks of Table 1, many more peaks will be recovered using a steady-state system.

Another problem the experiment suffers from is considerable background signal. Bremsstrahlung is believed to be a major cause of this problem.

RECOIL-RANGE STUDIES

In studying fission products shortly after fission, we have encountered the problem of identifying the elemental sources of the gamma rays. The normal way of attacking the species identification problem is to perform chemistry to separate fission products and to then observe the decay of the identified, separated elemental species. Project goals of obtaining defined spectra between 1 sec and a few minutes after fission would seem to preclude, at least for the shorter times, the chemical approach. Thus, an investigation of the possibility of using the physical separation associated with fission recoil has been made.

In the first experiment, a thin fission source (dissolved normal U) cast in cellulose acetate (approximately 3 microns thick) backed on a 6-micron Mylar film was used as a source of recoiling fission products. This film was sandwiched between other 6-micron Mylar films and irradiated in a GGA TRIGA reactor. About 1/2 hr after irradiation, or as soon as the films could be handled easily, the film package was undone and the two films, one, two, and three layers removed from the source film, were counted using the Ge-Li detector at appropriate time intervals. The source and film arrangement are shown in Fig. 1, and the results of these counts are presented as the ratio of counts in the second and third films corrected for radioactive decay losses (or gains) as a function of mass number.

Before describing the results, it is helpful to understand what might be expected to occur according to a slightly oversimplified model of this experiment. First, assuming the energy of a fission-recoil product is deposited linearly with distance through an absorber, a particular fission product originating at a point source would be stopped on the surface of an imaginary sphere in the absorber. The radius of the sphere is the recoil range for the particular fission product. If this sphere is intersected by equally spaced planes, the areas of the portions of the recoil sphere between these planes can be compared (i. e., area is proportional to the

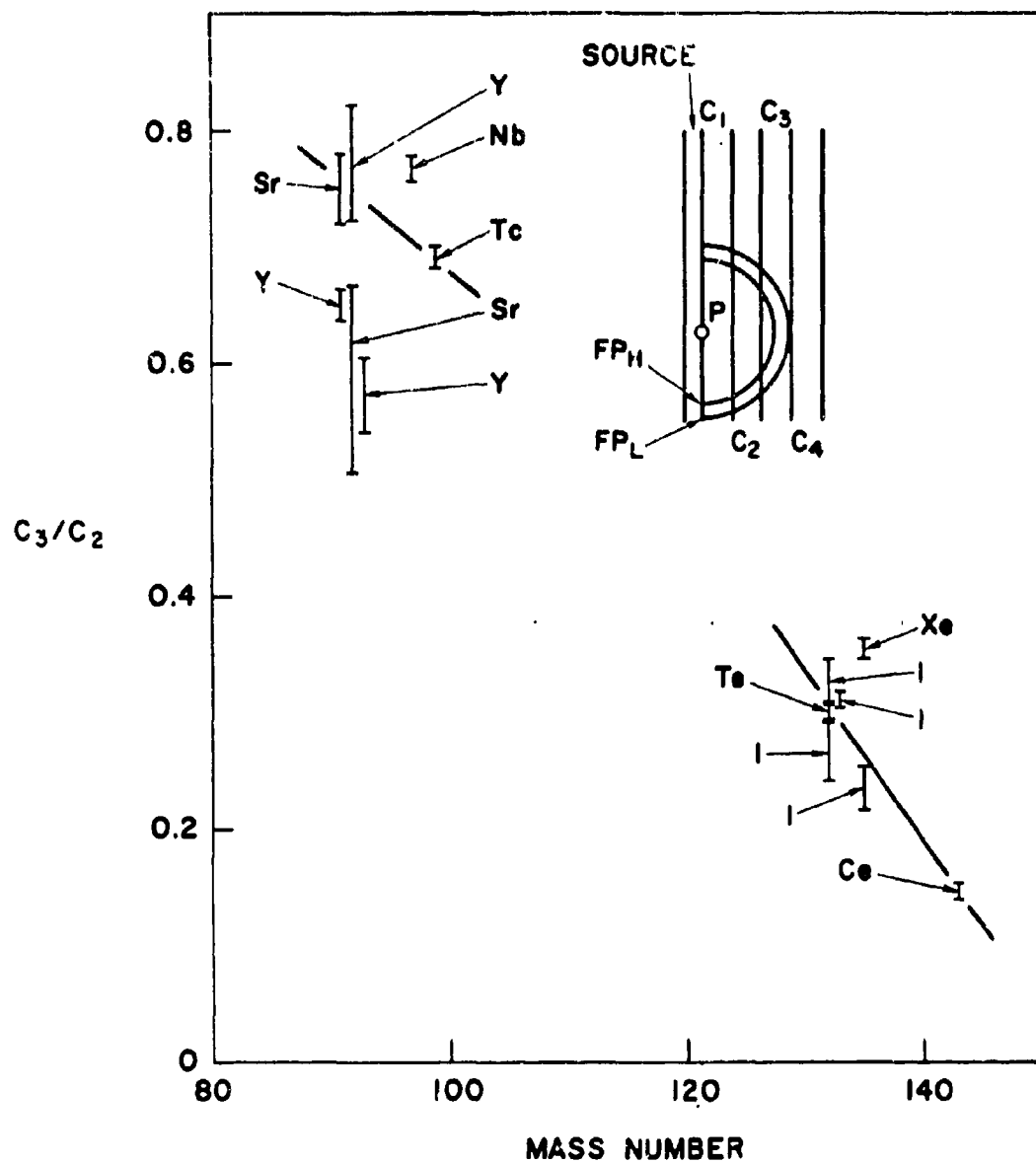


Fig. 1. Fission-product mass vs. recoil parameter

recoiled fission-product concentration). The area of the sphere between two planes will be the same as between another pair of equally spaced planes intersecting the sphere. The area between a plane intersecting the sphere and one that does not will be proportional to the distance between the last intersecting plane and a plane tangent to the sphere and parallel to the intersecting plane. Of course, a source plane is a multitude of source points with the above properties so that if the intersecting planes are parallel to the source plane, the above statements describe fission-product concentrations for this model. Finite thickness of the source plane alters the picture predictably. However, the plane source description is nearly true. In this model, then, fission-product recoil range may be distinguished by comparing the amount of a fission product in the last film that catches the fission product to the amount in a film nearer the source plane. Fission-product recoil-energy dissipation is not truly linear with distance; thus, precise range determinations are more complicated, but the real case parallels the above presentation.

Fission-product recoil range is mainly dependent on mass number of a fission product, its initial energy, and stopping properties of the medium in which recoiling takes place. In the nuclear scission process that produces a pair of fission products, each of the highly repelling nuclei attains a momentum of equal magnitude but opposite direction. The energy of fission is divided mainly into kinetic energy of these two particles. Generally, the lighter-fission products made in fission are more highly energetic and more penetrating. While this may not be universally correct, it is a good first approximation.

We have observed recoil-range variation with mass in our experimental measurements, as shown in Fig. 1. We believe that this curve is descriptive of the particular fission-product mass and that with better statistics we can achieve identification of a fission-product mass from its experimental recoil range within one or two mass units for a considerable range of masses. Gamma intensity data 10 hr after fission, presented in this figure, fall on the curve where the statistics are good. In some instances this relationship appears to fail. Where it does fail (as with Xe-135), we have found such experimental problems as unresolved gamma rays, which arise from two or more fission products of significantly different masses. This suggests that improvements in data processing are required.

A more extensive study of recoil range has been made. A series of Ge-Li gamma-ray spectra, made 42 min to 30 hr after a 60-min exposure of a sample in a GGA TRIGA reactor, has been produced. These spectra were obtained from recoil-fission products captured by stacked 6-micron Mylar films - in particular, in the second- and third-removed Mylar films from the U sample. In Fig. 2, a second-film-removed spectrum taken between 26 and 66 min after fission, is presented. The identities of most of

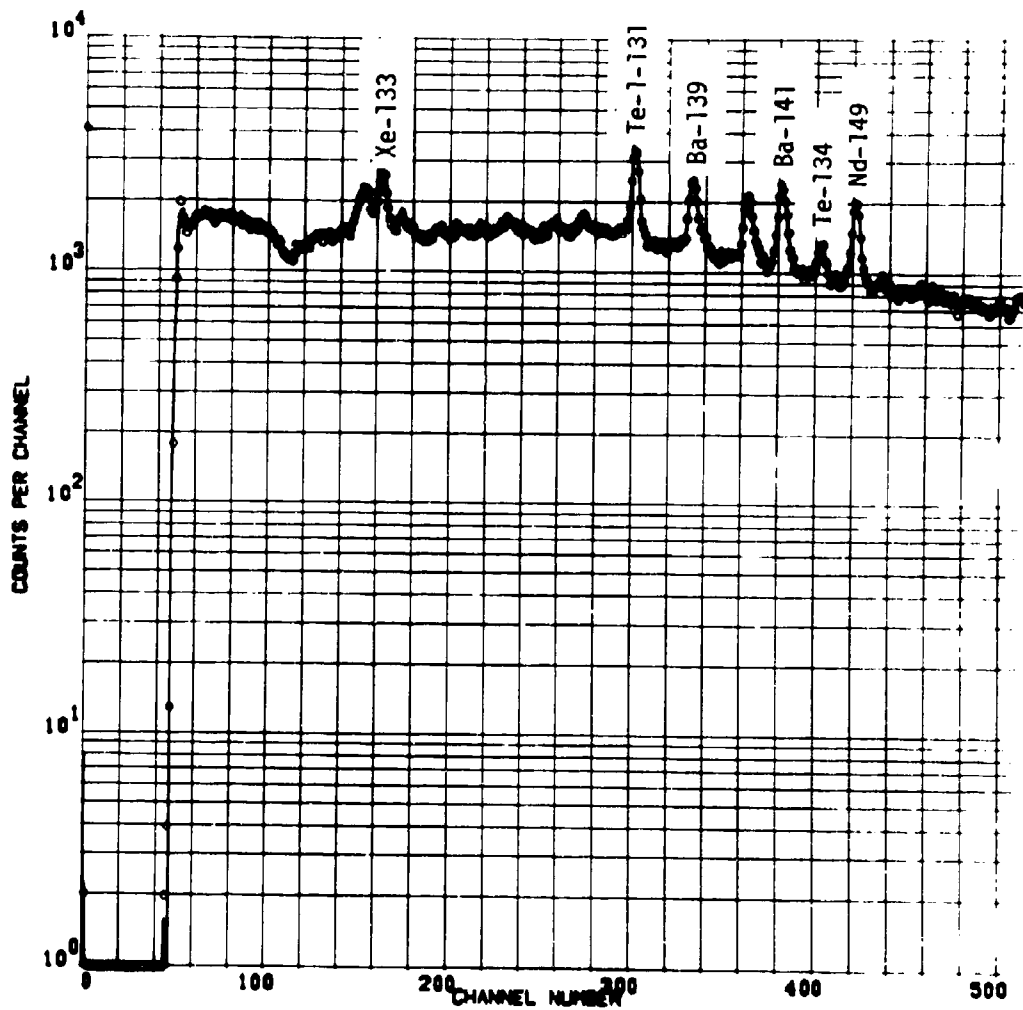


Fig. 2. Spectrum for second film taken 26 to 66 min after fission (1-hr irradiation) (Sheet 1 of 8)

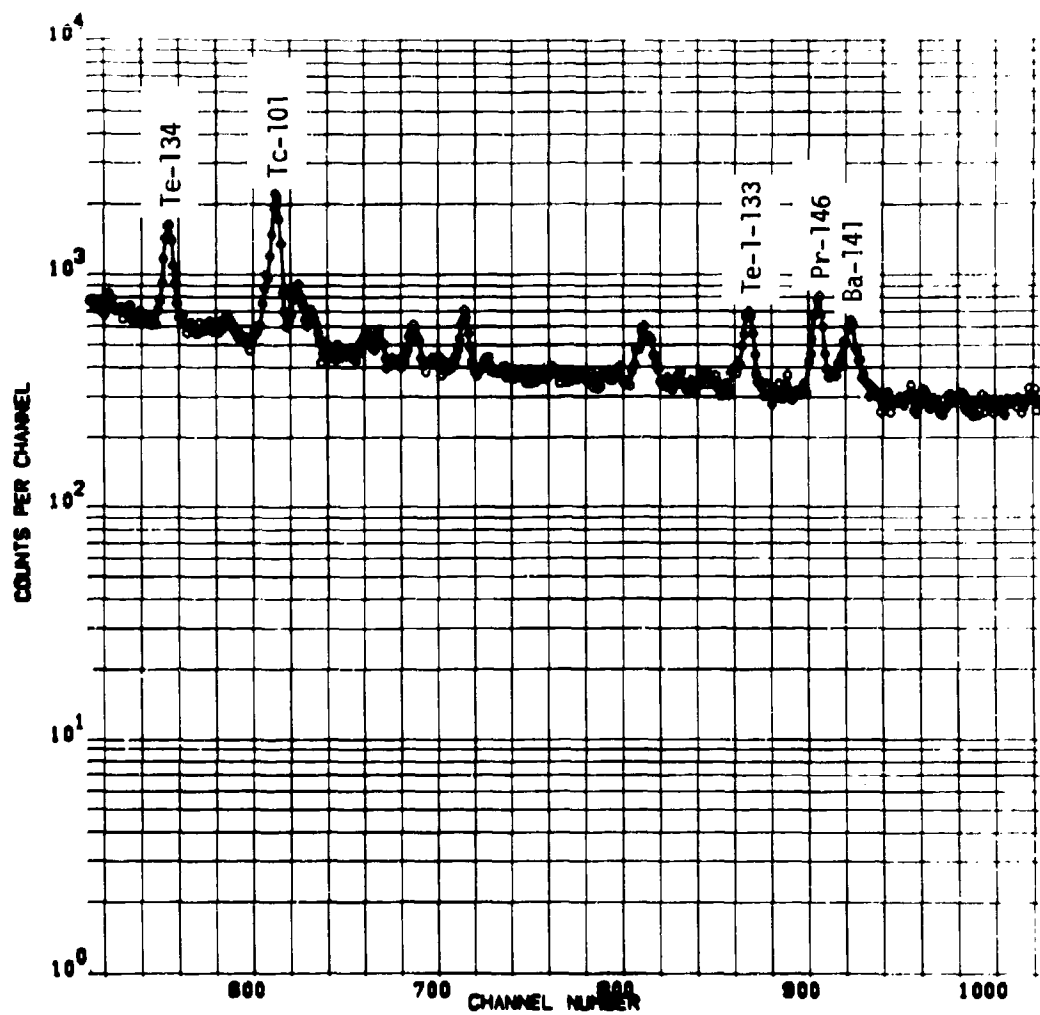


Fig. 2. Spectrum for second film taken 26 to 66 min after fission (1-hr irradiation) (Sheet 2 of 8)

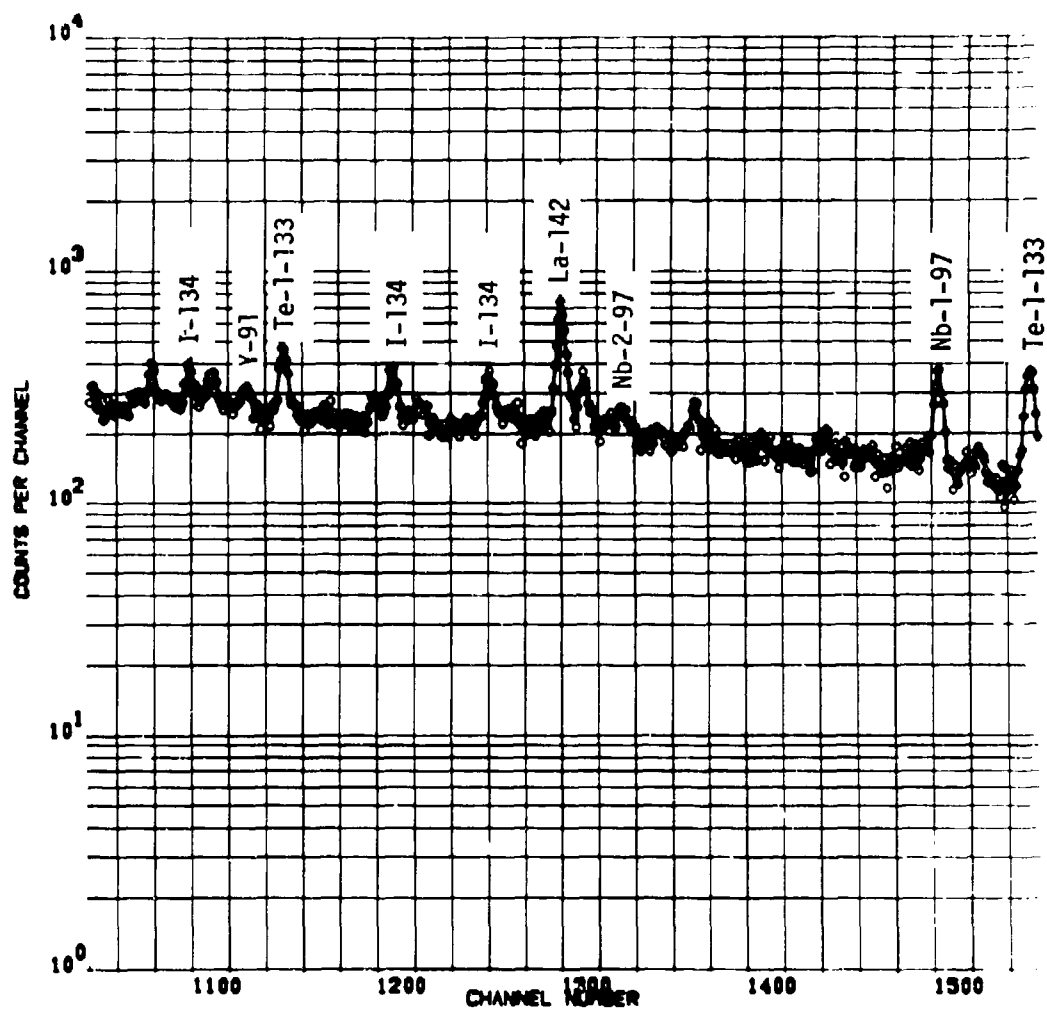


Fig. 2. Spectrum for second film taken 26 to 66 min after fission (1-hr irradiation) (Sheet 3 of 8)

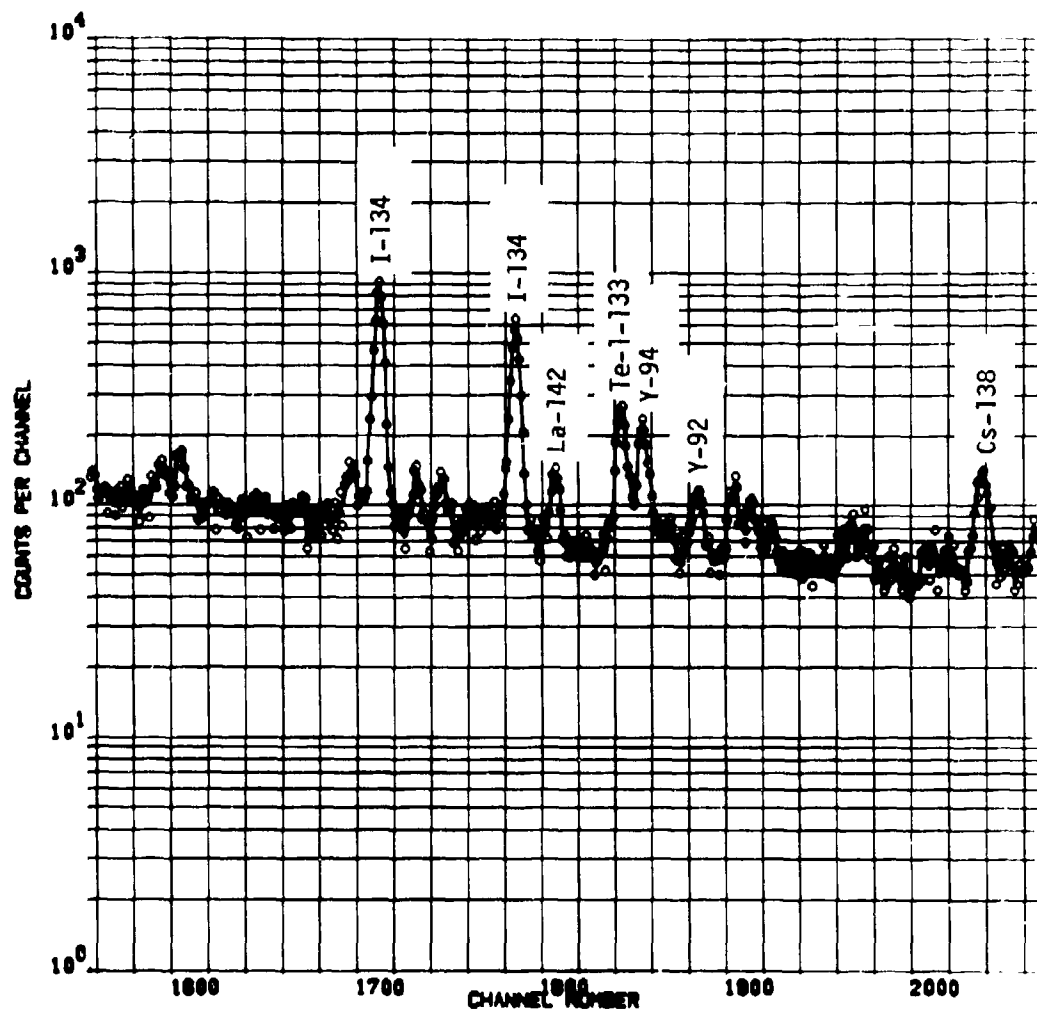


Fig. 2. Spectrum for second film taken 26 to 66 min after fission (1-hr irradiation) (Sheet 4 of 8)

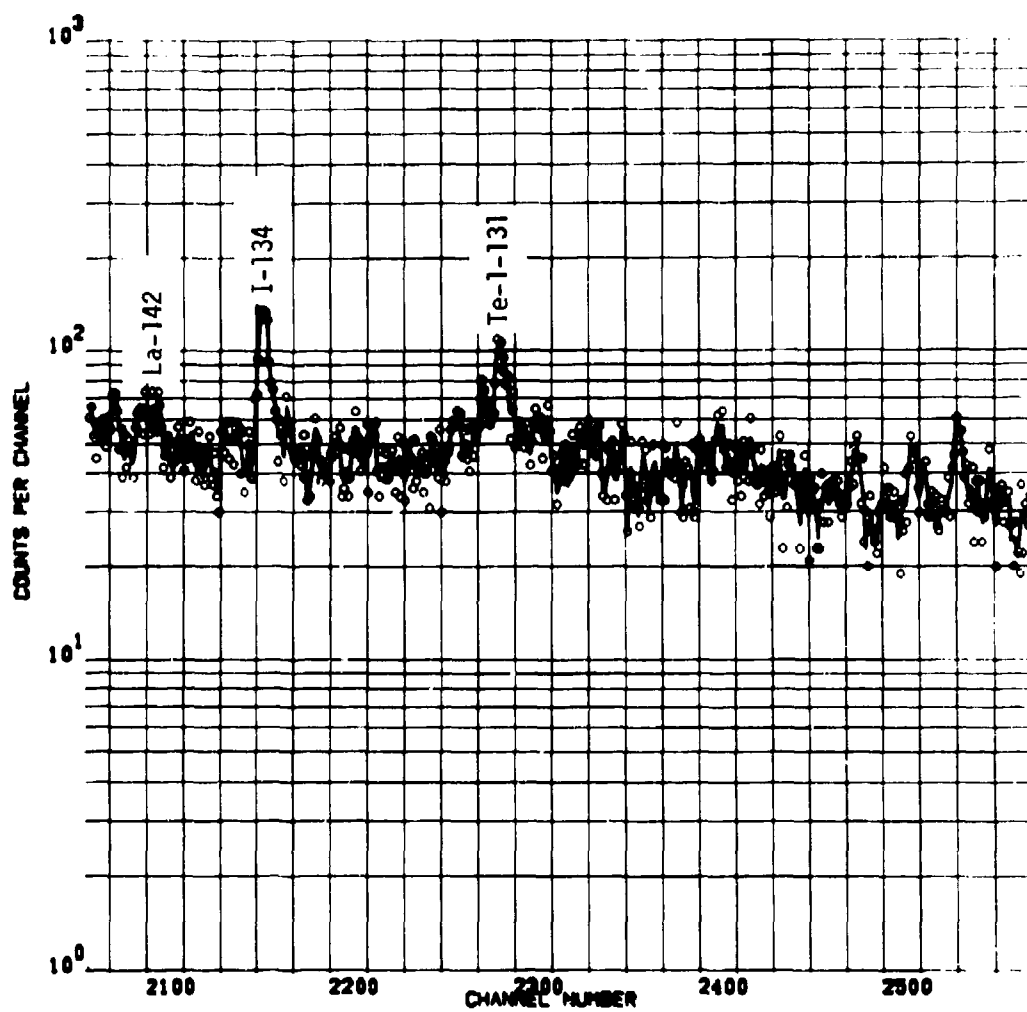


Fig. 2. Spectrum for second film taken 26 to 66 min after fission (1-hr irradiation) (Sheet 5 of 8)

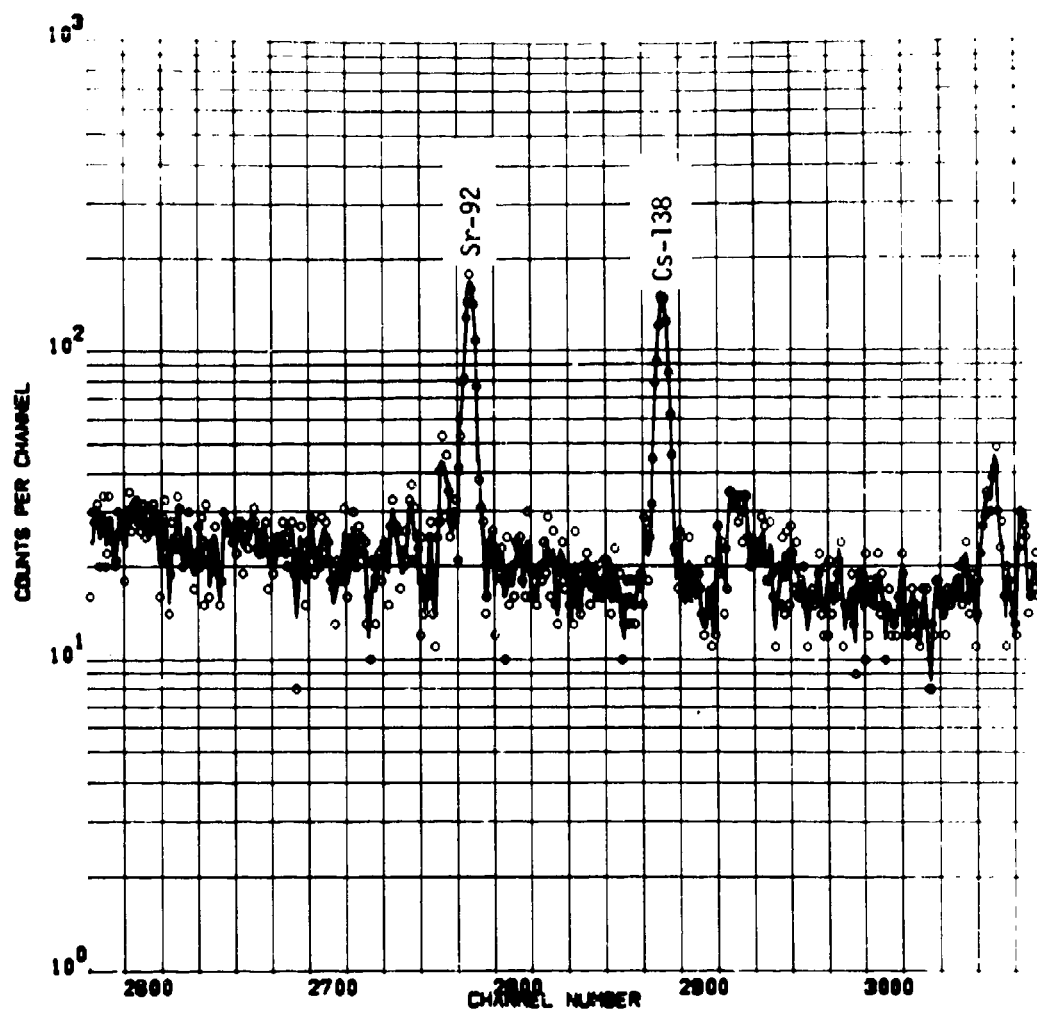


Fig. 2. Spectrum for second film taken 26 to 66 min after fission (1-hr irradiation) (Sheet 6 of 8)

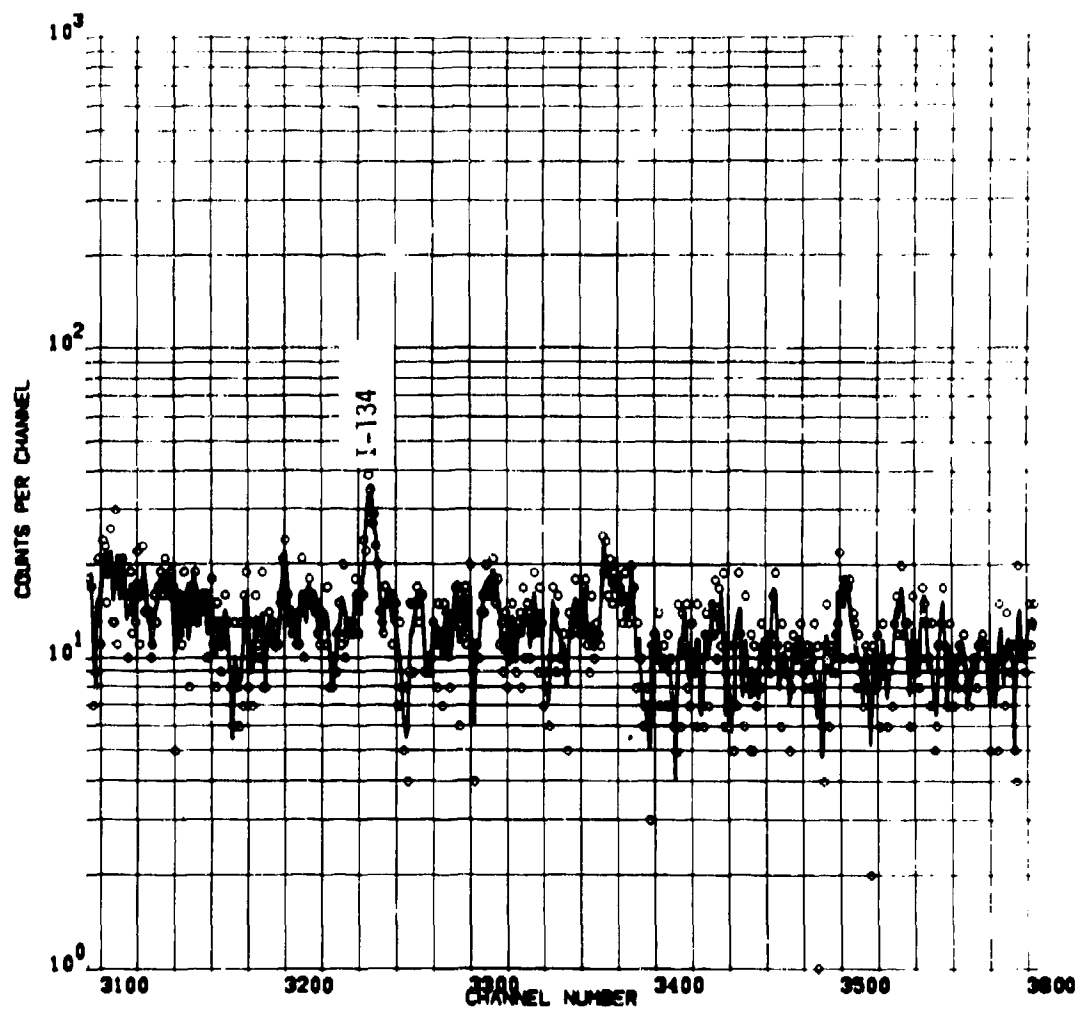


Fig. 2. Spectrum for second film taken 26 to 66 min after fission
(1-hr irradiation) (Sheet 7 of 8)

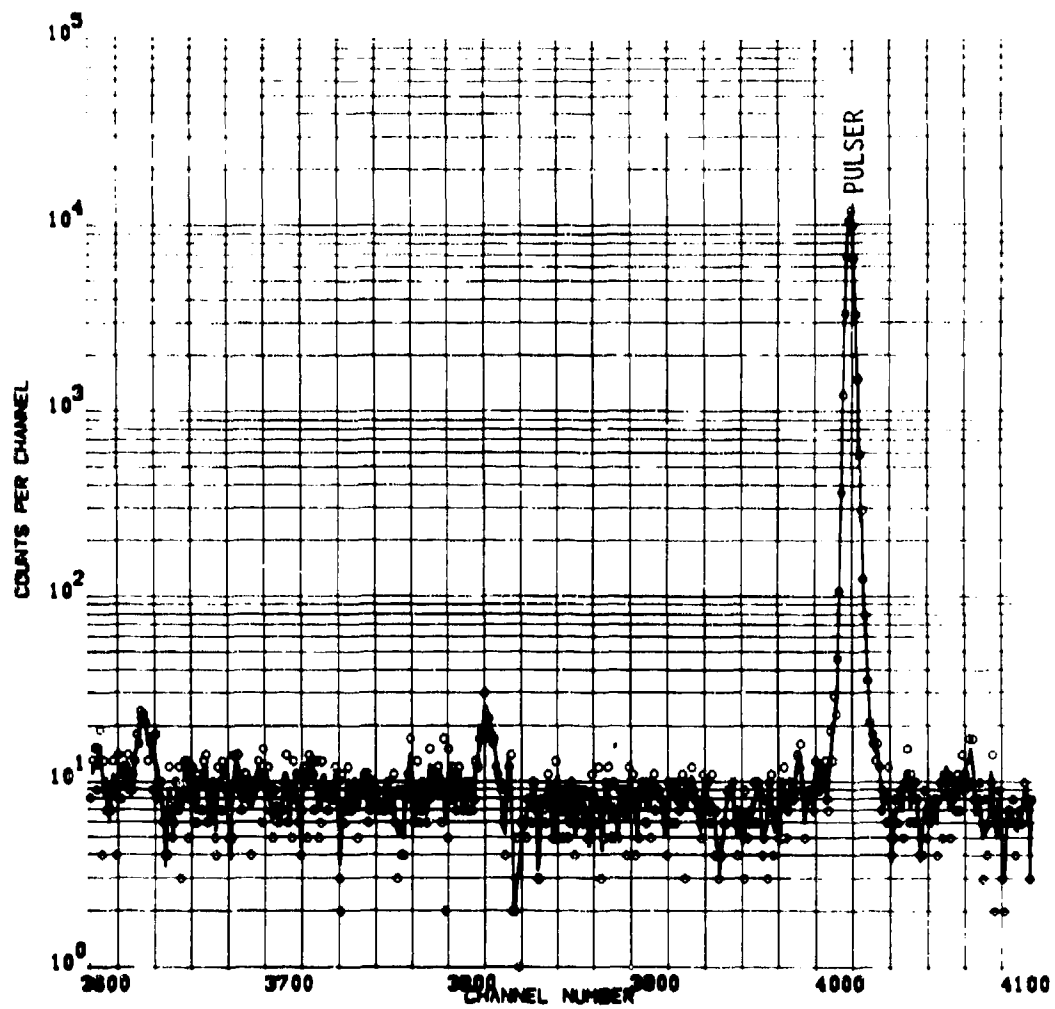


Fig. 2. Spectrum for second film taken 26 to 66 min after fission
(1-hr irradiation) (Sheet 8 of 8)

the peaks in this spectrum are called out, although a few of these identifications are tenuous. The identifications that have been made are in agreement with the anticipated recoil ranges and half-lives of the fission products within the accuracy permitted by the counting data. The data from this experiment (this spectrum and nine others) are presented in Table 2 as a gamma energy, a peak intensity ratio in the third and second films, an apparent half-life, and an isotope identification where an assignment has been made. While there may be a few assignment errors, there has been a great deal of success using the film intensity ratio in helping to establish the assignment. The problem of proper unfolding of closely spaced gamma lines remains.

As a further demonstration of the recoil-range measurements, C_3/C_2 ratios for I-135 at five different times after irradiation were measured. The results are presented in Fig. 3. The I-135 peak intensities were too weak at the first time measured and are not shown. The data at the second and fifth measured times are marginal although shown on the graph. The deviation bars are calculated standard deviations, σ , according to counting statistics. Dropping four points because of suspected bias (more should be dropped), 60% of the data fall within one σ of $C_3/C_2 = 0.338$ and 85% within two σ . These values should statistically be 68% and 95%, respectively. The very accurate data points (2.5% σ or less) that are necessary for the projected studies are in good agreement with this value.

The best data on heavy-mass-fission products are presented in Fig. 4. These data certainly suggest that recoil range can be used for nuclide identifications in the reported range provided the relationship between the nuclide number and C_3/C_2 is monotonic — a line is used to describe the data in the figure. The data define the selected line within one mass unit, suggesting that with good count data a nuclide's mass number can be identified from its C_3/C_2 values in this region, plus or minus one atomic mass unit.

STEADY-STATE SHORT-LIVED FISSION-PRODUCT STUDIES

The requirements for making an extensive, accurate study of short-lived fission products can be enumerated. First, one must observe a sufficient number of fission-product decay events at several times after fission so an accurate mathematical description of birth and decay of fission products can be obtained. Of course, sufficient energy resolution of these gamma counts into a specific disintegration process must be possible. Second, a method of associating particular isotopic disintegrations with each observed set of count data associated with a particular gamma energy must be available. The first requirement is best satisfied by making steady state studies of fission-product decay using a Ge-Li detector and an appropriate multichannel analyzer (4096 channels). Using

TABLE 2

FISSION-PRODUCT GAMMA-ENERGY/RECOIL-RANGE CORRELATION

Energy (KeV)	C_3/C_2	$t_{1/2}$ (hr)	Isotope	Energy (KeV)	C_3/C_2	$t_{1/2}$ (hr)	Isotope
1917	0.9	13	Y-93	947		1.2	
1901		1.1		933	0.91	4	Y-92
1806	0.26	0.8		924	0.85	11	Y-93
1791	0.33	5.4	I-135	917	0.86		Y-94
1750		Long		912	0.36	1.6	Te-1-133
1731				894	0.2	1	La-142
1706	0.35	6	I-135	883	0.37	1.0	I-134
1678	0.334	6.5	I-135	875	0.5	22	I-133
1613	0.34	1	I-134	863		1.7	
1596	0.24	Long	La-140	856			
1566	0.5			846	0.39	1.1	I-134
1503	0.65	4		836	0.32	6.5	I-135
1457	0.34	6	I-135	812	0.46	4.4	
1435	0.245	0.9	Cs-138	793		1.9	
1405	1.0	4.7	Y-92	772	0.38		I-132
1398	0.39		I-132	766	0.39	1.5	Te-1-133
1384	0.908	2.7	Sr-92	755		Long	Zr-95
1369	0.6	11	Kr-88	749	0.88	10.5	Sr-91
1354		2.3		742	0.80	17	Nb-1-97
1298	0.42	22		723	0.6	7.2	Ru-105
1281		5		692	0.9		
1260	0.34	6.6	I-135	667	0.40	Long	I-132
1240		6		657	0.87	17	Nb-2-97
1236	0.6			646	0.35	1.2	
1160			I-134	640	0.200	1.4	La-142
1147	0.78	12	Zr-97	629		Long	
1142		2.7		620	0.4	1.3	I-134
1135	0.4		Te-1-131	601	1.1	Long	
1131	0.34	6.5	I-135	594			I-134
1124	0.4	6.8	I-135	564	0.39		Te-1-133
1071	0.4	1.1	I-134	554	0.897	12	Y-91
1043		1.5	La-142	545	0.37	6.5	I-135
1038	0.33	6.7	I-135	539	0.34		I-134
1023	0.879	10	Sr-91	536	0.28	Long	Ba-140
1010	0.24	1.2	Cs-138	529	0.37	15	I-133,
977		1.5					Xe-1-135
971	0.2	7.4		510	0.21	2.5	
953			I-132	507	0.7	16	Zr-97

TABLE 2 (continued)

Energy (KeV)	C_3/C_2	$t_{1/2}$ (hr)	Isotope	Energy (KeV)	C_3/C_2	$t_{1/2}$ (hr)	Isotope
496	0.82	Long	Ru-103	266	0.9	10	Y-93
488	0.1	2		253		Long	Zr-97
468	0.8	4.4	Ru-105	249	0.28	7	Xe-2-135
461	0.22	Short	Ba-141	240	0.9	3	
452	0.22	Short	Pr-146	228	0.388	Long	Te-132
447	0.8	3	Y-92	220	0.3	6.8	I-135
433	0.3	1.9	Te-1-133	211	0.25	1.3	Nd-149
430	0.6	1.6	Sr-92	201	0.39	0.8	Te-134
423	0.3	2.3		190	0.29	0.5	Ba-141
417	0.38	7	I-135	181	0.42	1	
405	0.5	1.2		167	0.25	1.6	Ba-139
392		1.4	I-134	156		2	
385			I-132	150	0.4	0.9	Te-1-131
364	0.5	Long	I-131	142	0.85	Long	Tc-99
357	0.88	Short		129	0.5		Rh-105
354		13		116		2	
343	0.4	Short		105	0.1		
318	0.65		Rh-2-105	92			Nd-147
311	0.56	1.3		86		2	
306	0.71	0.5	Tc-101	81		Short	Xe-133
293	0.21	Long	Ce-143	76		2	
277	0.35	1.0	Te-134	59		30	
274	0.4	17		50	0.3	5	

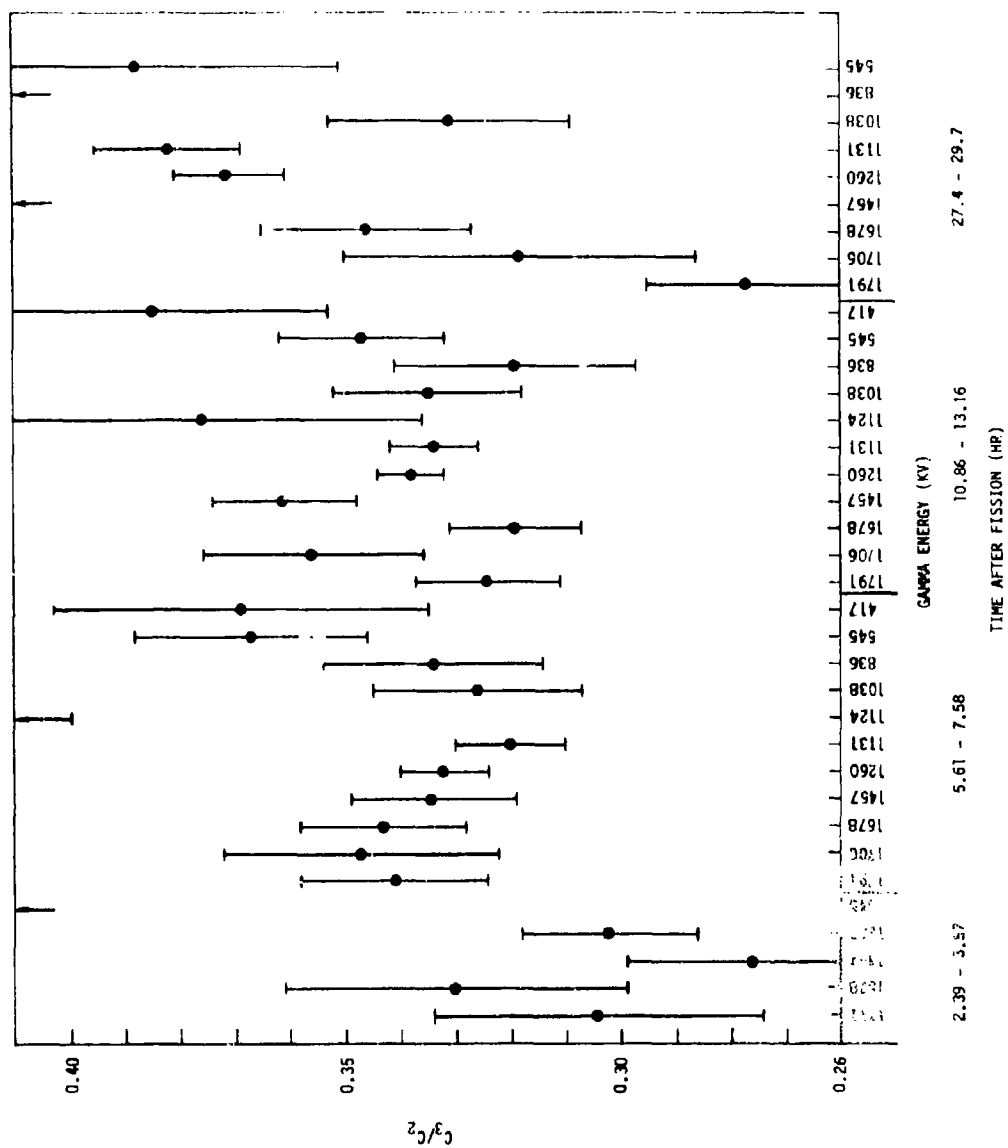


Fig. 3. Recoil-range parameters at various times for the observed spectral lines of I-135

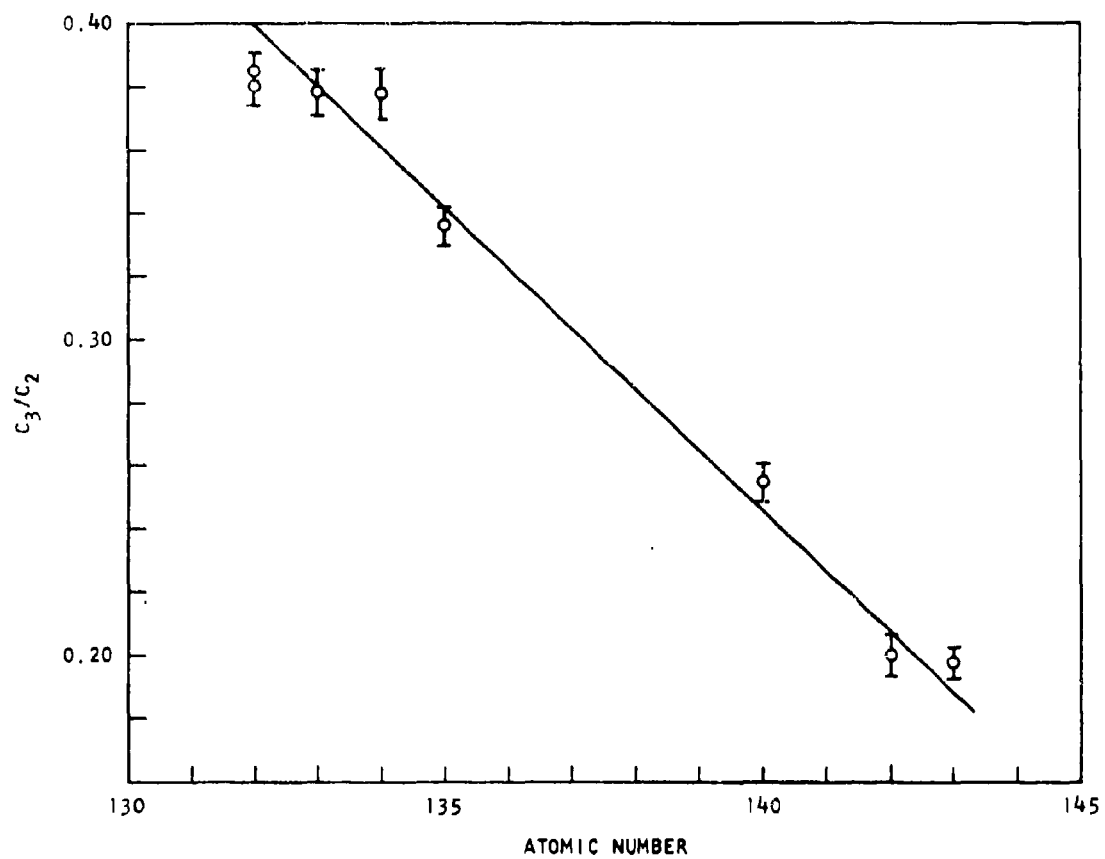


Fig. 4. Fission-product recoil-range parameter C_3/C_2 in Mylar vs. atomic mass

a steady-state system one would be able to observe the gamma radiation from fission products a set delay time after birth for a long period. This observation can be accomplished by allowing recoil of fission products to separate fuel and fission products, catching the recoils in some medium and studying the decay of these recoiled fission products. The second requirement can be satisfied by using measured recoil ranges associated with the established gamma energies to aid in identifying the fission-product emitting the observed gamma ray.

A system that should make measuring steady-state recoil range and half-lives possible is shown diagrammatically in Fig. 5. Two thin Mylar tapes pass in front of a recoiling fission-product source. To determine the recoil range associated with a particular gamma ray, the counting rates in the two films need to be well established at a particular time after fission. This will be done by passing each film containing recoiled fission products from the steady-state fission source in front of a detector at a specific delay time after fission and continuously counting more or less of the moving film until statistically adequate count rates of fission products can be established. Once recoil range and, accordingly, gamma-ray identifications are made, one of the recoil target films will be counted at various delay times after fission to provide a measure of specific short-lived isotope concentration versus time. From these data, half-lives of the short-lived fission product (1 to 100 sec) can be derived. From these measured half-lives and initial yields, the quantities of individual fission products as a function of time will be better established for fractionation estimations.

Equipment for these studies, involving either neutron-beam tube fission studies or Cf-252 spontaneous fission studies or both, has been designed and will be built and used as part of a new contract.

UNFOLDING GAMMA-RAY SPECTRA

The various gamma rays of fission products shortly after fission are so abundant that measured spectra lines exhibit considerable overlap, even with an energy resolution of 2.8 KeV (energy band width at one-half peak intensity). Most of the data reported here had resolution of that order, as shown in Fig. 2. The studies made so far require complex computer processing for roughly one-half of the observed peaks to obtain reliable estimates of total counts under a peak. For the purpose of obtaining reliable total counts from these overlapping spectra, a portion of our effort has been expended to establish a least-squares fit to a gamma-ray spectrum in the form of sums of Gaussian distributions and an exponential background function. The system has provided reasonable description of some peak complexes, but it requires optimization and further testing.

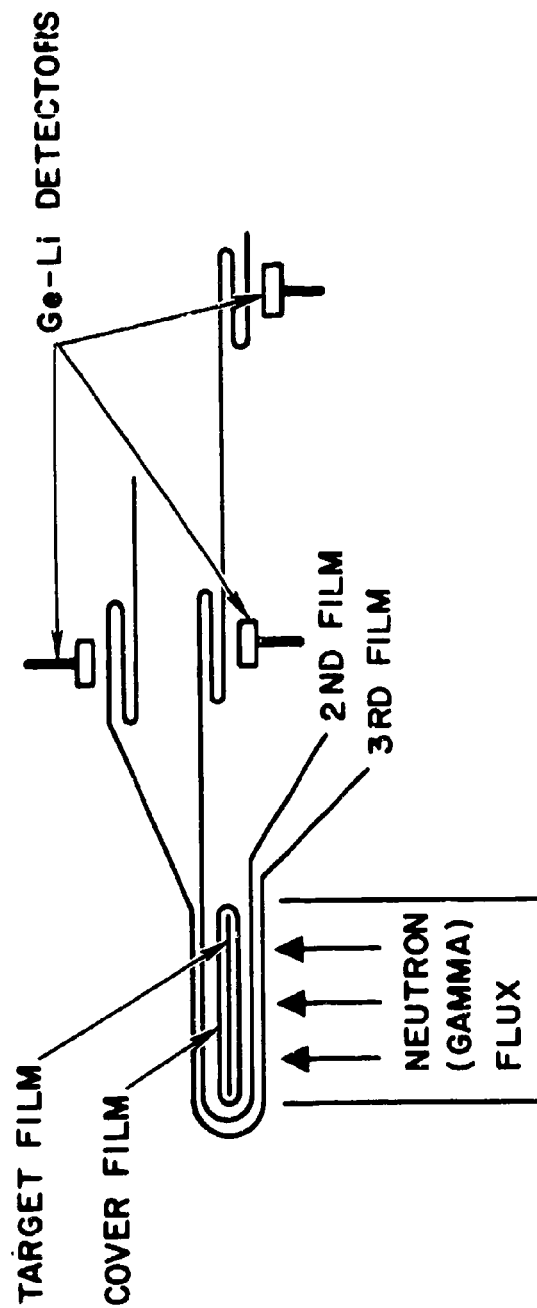


Fig. 5. Steady-state recoil fission-product experiment

The data-processing system presently used is not entirely satisfactory for the work we are trying to accomplish, particularly since peak areas accurate to better than $\pm 5\%$ are essential to the recoil-range identification studies.

DIFFUSION OF RADIONUCLIDES IN MOLTEN SILICATES

The diffusion of fission-product nuclides in molten silicate matrices is of major importance in any realistic model for fallout formation. (2, 3) We have continued our investigations of this phenomenon. Studies of the diffusion of radiosodium and radioantimony in molten matrices from the sodium disilicate-albite system have been completed. An investigation of the diffusion of radioantimony in molten Nevada soil has been performed. The simultaneous diffusion of several radionuclides in molten media from the $\text{CaO-Al}_2\text{O}_3\text{-SiO}_2$ system has been studied using two different techniques. The latter study was made possible by the availability of a 4096-channel gamma analyzer and a high-resolution Ge-Li detector. The experiments have helped to clarify the role of silicate composition in diffusion.

DIFFUSION IN THE $\text{Na}_2\text{O-Al}_2\text{O}_3\text{-SiO}_2$ SYSTEM

The use of a condensed-state diffusional model to predict fractionation in fallout requires knowledge of diffusion rates in fallout matrix material. Most of the diffusion studies performed at GGA have been concerned with the $\text{CaO-Al}_2\text{O}_3\text{-SiO}_2$ system. Methods of predicting diffusivities have been developed and tested for this system. For estimating fractionation during fallout formation, it would appear necessary to at least test diffusion-coefficient estimation methods on other systems. This has been partially accomplished in studies of the $\text{Na}_2\text{O-Al}_2\text{O}_3\text{-SiO}_2$ system.

For these investigations, four compositions from the $\text{Na}_2\text{O-Al}_2\text{O}_3\text{-SiO}_2$ ternary system were chosen. These silicates were 100% albite ($\text{Na}_2\text{O} \cdot \text{Al}_2\text{O}_3 \cdot 6 \text{SiO}_2$), 100% sodium disilicate ($\text{Na}_2\text{O} \cdot 2 \text{SiO}_2$), and 38:62 and 60:40 mixtures of these silicates. This particular system was chosen for several reasons. Albite, a common mineral, can be considered representative of a medium refractory soil for fallout simulation, and sodium disilicate is representative of a low refractory soil. Also, there are data reported for the leaching of radiocesium-diffused albite. (4) From the latter, and using the results of the present study for Na, predictions of diffusivities of several other radionuclides can be made for the molten albite composition. This will be discussed in detail below. Finally, this system was chosen to study the problem of precrystalline structure, or configurational entropy effect, in molten silicates.

The first part of this study was concerned with the self-diffusion of radio-sodium in the molten matrices. The sources that were used for the plane source technique⁽³⁾ were prepared by activating the silicates in a GGA TRIGA reactor to yield Na-24. Six experiments were completed in the temperature range of 1072° to 1661° K. These points are superimposed on the phase diagram reported by Schairer and Bowen⁽⁵⁾ that is approximately reproduced in Fig. 6. The first four experiments with the 38:62 and 60:40 matrices were completed. These four diffusivity values were then combined with the results for the diffusion of Na in sodium disilicate that were reported by Malkin and Mogutnov⁽⁶⁾ to establish the compensation law for this system.⁽³⁾ The latter was obtained by treating the data by the method of least-squares to yield

$$\log_{10} D_0 = -4.33 + 0.123 E^* \quad , \quad (1)$$

where D_0 and E^* are the preexponential factor (cm^2/sec) and activation energy (kcal/mole), respectively, in the Arrhenius equation for diffusion. An experiment was then done with sodium disilicate to compare with the results of Malkin and Mogutnov. At 1248°K, the experimental value was found to be $1.4 \times 10^{-5} \text{ cm}^2/\text{sec}$, which compared well with the value of $1.5 \times 10^{-5} \text{ cm}^2/\text{sec}$ calculated from the equation reported by Malkin and Mogutnov. An empirical correlation was then found between E^* and the percent albite composition, and E^* was predicted for the 100% molten albite composition by extrapolation. Using Eq. 1, D_0 was found for that matrix and an experiment was done at 1661° K. The experimental value of the diffusivity was found to be $1.6 \times 10^{-5} \text{ cm}^2/\text{sec}$, which compared well with the predicted value of $2.5 \times 10^{-5} \text{ cm}^2/\text{sec}$. This result substantiated the empirical correlation mentioned above. The experimental results are summarized in Table 3.

TABLE 3
DIFFUSIVITIES FOR TRANSPORT OF Na-24 IN
MELTS FROM THE SODIUM DISILICATE-ALBITE SYSTEM

T (° K)	Composition (% Albite) ^(a)	$D \times 10^6$ (cm^2/sec)(b)
1072	38	2.8
1248	38	6.9
1365	60	9.8
1248	60	5.0
1248	0	14.
1661	100	16.

(a) The uncertainty is approximately 2%

(b) The uncertainty is approximately 50%

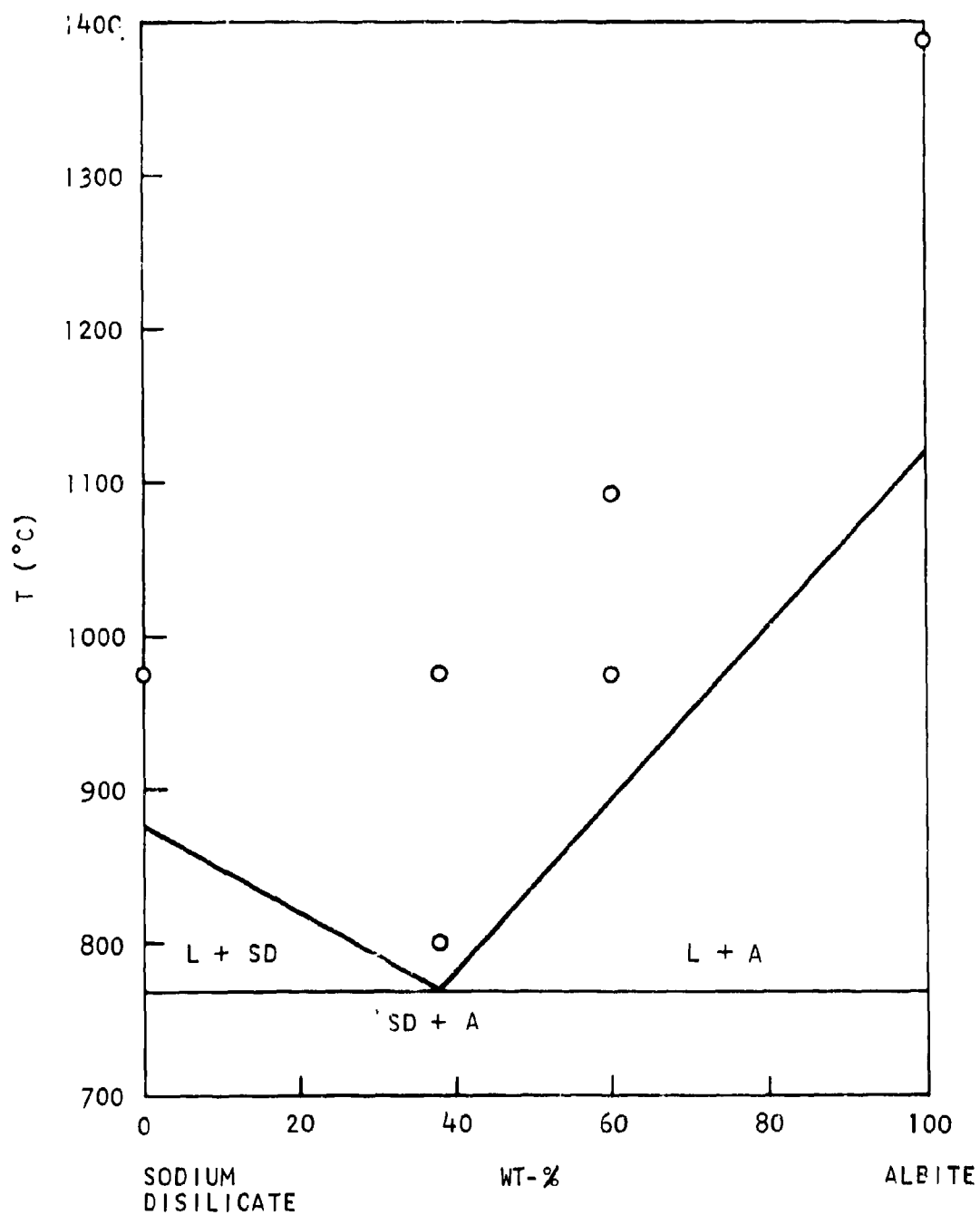


Fig. 6. Phase diagram for the sodium disilicate-albite system showing parameters of diffusion experiments

The Arrhenius parameters for this system are summarized in Table 4.

TABLE 4

ARRHENIUS PARAMETERS FOR DIFFUSION OF Na-24 IN
MELTS FROM THE SODIUM DISILICATE-ALBITE SYSTEM

Composition (% Albite)	E^* (kcal/mole)	$\log_{10} D_0$ (D_0 in cm^2/sec)
0	11.9 ^(a)	- 2.74 ^(a)
38	13.5 \pm 1.0 ^(b)	- 2.67 ^(d)
60	19.5 \pm 1.0 ^(b)	- 1.93 ^(d)
100	32.3 \pm 1.5 ^(c)	- 0.36 ^(c)

- (a) From Malkin and Mogutnov⁽⁶⁾
- (b) Uncertainties estimated from Eq. 1
- (c) From empirical correlation and Eq. 1
- (d) From Eq. 1

Using the results obtained for the diffusion of Na in the molten albite together with the leaching data for the radiocesium-diffused melts of albite composition reported by Lane,⁽⁴⁾ it was possible to predict diffusivities for several species in this matrix. Lane allowed Cs to diffuse into the matrix at different temperatures above the liquidus. He then leached the samples using 0.1 N HCl. From his data E^* for the diffusion of Cs into the matrix is estimated to be 36.6 kcal/mole. It has been shown⁽³⁾ that E^* (or $\log_{10} D_0$) is a linear function of the reciprocal ionic radius, r^{-1} ,

$$E^* = a + br^{-1} \quad (2)$$

for the alkali metals and I in those cases where sufficient data exist. For the present case, the coefficients in Eq. 2 were determined using the values of E^* for Cs and Na. The values of E^* for I, Rb, K, and Li were then calculated. Equation 1 was then used to calculate the corresponding values of $\log_{10} D_0$. These results are summarized in Table 5.

TABLE 5

EXPERIMENTAL AND PREDICTED ARRHENIUS PARAMETERS
FOR DIFFUSION IN MELTS OF ALBITE COMPOSITION

Nuclide	E* (kcal/mole)	$\log_{10} D_0$ (D_0 in cm^2/sec)
I	37.8	0.32
Cs	36.6	0.17
Rb	35.8	0.07
K	35.1	- 0.01
Na	32.3	- 0.36
Li	26.5	- 1.07

It is emphasized that the values reported in Table 5 are estimates for all of the nuclides except Na. The estimates are, however, based on a rational approach to the problem of predicting diffusivities. It is anticipated that the prediction will be tested experimentally for at least one nuclide.

A study of the diffusion of radioantimony in molten media from the sodium-disilicate-albite system has been completed. The temperature range for the experiments was 1123° to 1687°K. Experimental techniques were identical with those described for the diffusion of Na in this system. The results are listed in Table 6.

The character of the soil that might be involved in a near-earth detonation is critical to fractionation calculations. If condensed-state diffusion is a limiting factor in the formation of fallout particles, and we believe it is at least one of the important factors, then orders of magnitude in the diffusivity as demonstrated in the data of Table 6 become important. The data are also presented in Fig. 7 where the diffusivity is plotted on a logarithmic scale as a function of the reciprocal temperature.

The experiment at 1344°K using the eutectic matrix was performed, and then, using the compensation law as defined by the data for the albite and sodium-disilicate compositions, the diffusivity in the eutectic matrix at 1120°K was predicted. The predicted value was identical to the experimental value of $2.1 \times 10^{-8} \text{ cm}^2/\text{sec}$ at 1123°K. The result was consistent with the assumption of compensation for this system. The results are summarized in Table 7.

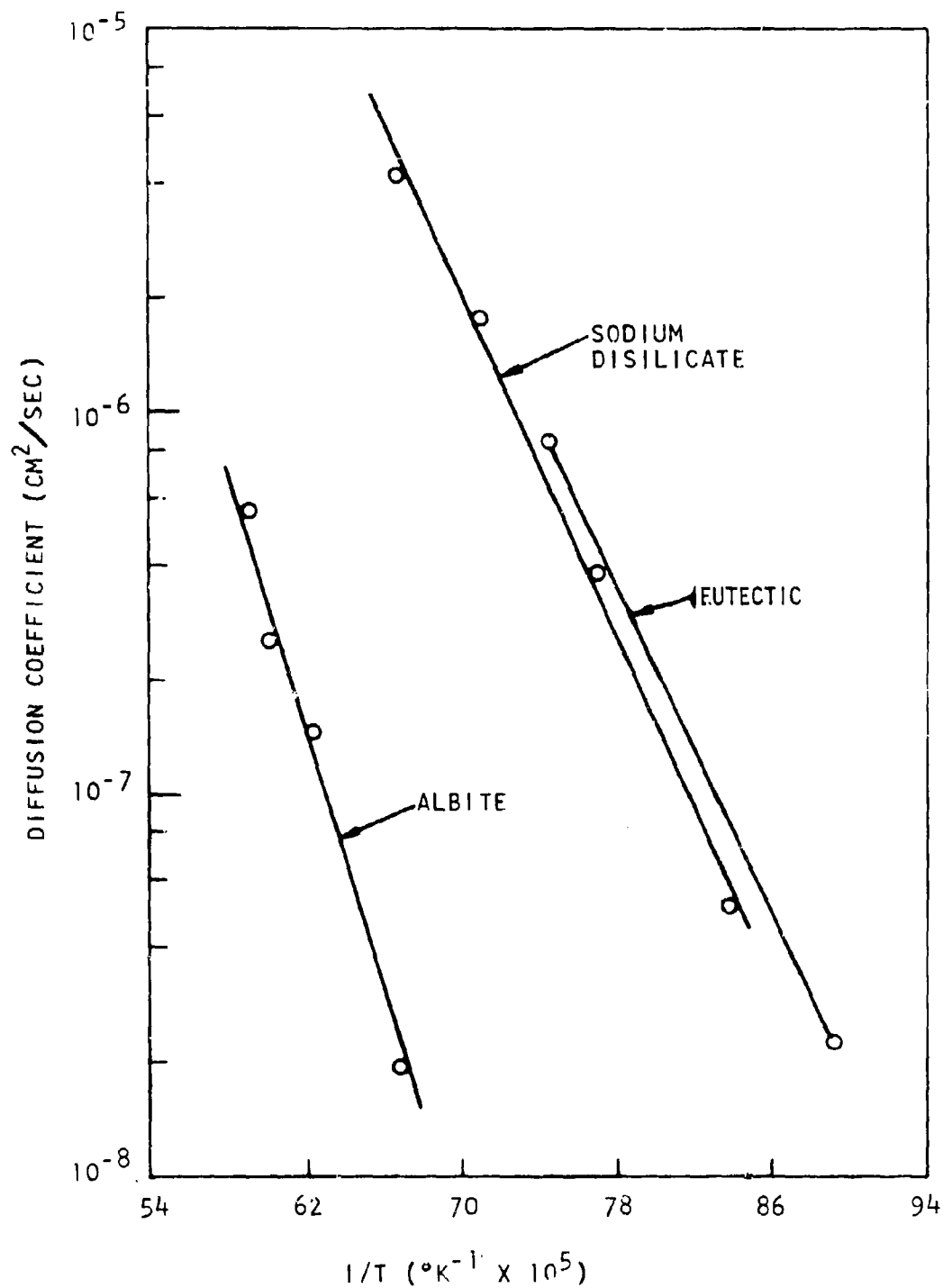


Fig. 7. Diffusion coefficients for the transport of Sb-124 in liquids from the sodium disilicate-albite system as a function of temperature

TABLE 6

DIFFUSION COEFFICIENTS FOR THE TRANSPORT OF RADIOANTIMONY
IN LIQUIDS FROM THE SODIUM DISILICATE-ALBITE SYSTEM

Matrix	T (°K) ^(a)	D × 10 ⁸ (cm ² /sec) ^(b)
Albite	1687	55
Albite	1657	25
Albite	1599	15
Albite	1499	1.9
Sodium Disilicate	1495	410
Sodium Disilicate	1407	170
Sodium Disilicate	1301	37
Sodium Disilicate	1195	5.1
Eutectic	1344	86
Eutectic	1123	2.1

(a) The uncertainty is approximately 10°K

(b) The uncertainty is approximately 20%

TABLE 7

ARRHENIUS PARAMETERS FOR Sb-124 DIFFUSION IN MELTS
FROM THE SODIUM DISILICATE-ALBITE SYSTEM

Composition (% Albite)	E* (kcal/mole)	log ₁₀ D ₀ (D ₀ in cm ² /sec)
0	52.2	2.29
38	50.8	2.20
100	87.6	5.06

In Fig. 8, the energies of activation for diffusion of Na and Sb are compared with the sodium-disilicate phase diagram. It is emphasized that all of these experiments were conducted in the liquidus region. For both Na and Sb it appears that there is at least a qualitative reflection of the phase diagram by the activation energy. This effect, although evident, is not as

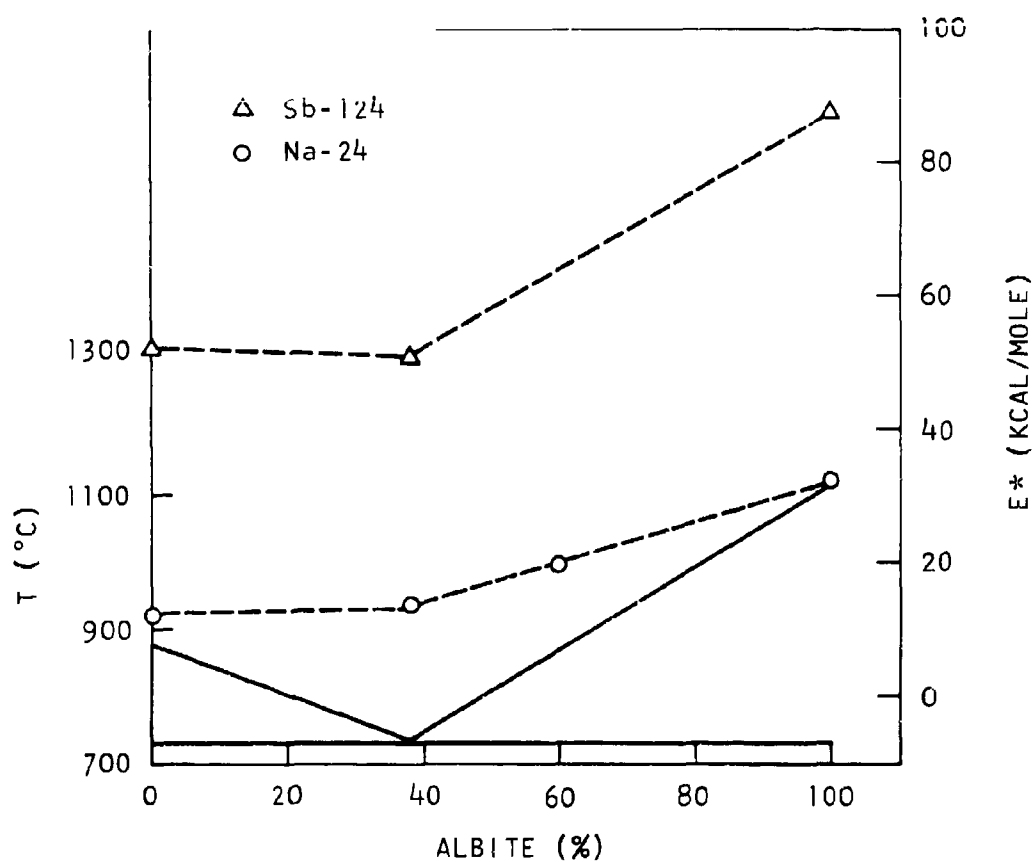


Fig. 8. Comparison of energies of activation for diffusion in molten media with the sodium disilicate-albite phase diagram

pronounced as that found for the $\text{SbO}_x\text{-CaO-Al}_2\text{O}_3\text{-SiO}_2$ system.⁽³⁾ However, the data show evidence of precrystalline structure in the liquidus. This effect has been observed in several other silicate systems, for example, in the $\text{Na}_2\text{O-SiO}_2$ system by Dertev and Voronkova.⁽⁷⁾ Their data for the diffusion of Na in these molten silicates reflect the equilibrium phase diagram; i. e., maxima for the diffusivity appear at two eutectics and at the composition corresponding to $\text{Na}_2\text{O} \cdot 2 \text{SiO}_2$. This interesting problem deserves further attention and we anticipate conducting experiments to further define it.

DIFFUSION IN MOLTEN NEVADA SOIL

An investigation of the diffusion of radioantimony in molten Nevada soil taken from the Small Boy detonation site was completed. The purpose of the study was to make a second comparison of Nevada soil with the $\text{CaO-Al}_2\text{O}_3\text{-SiO}_2$ eutectic, which is the reference matrix used in the GGA laboratory.

Sixty-day Sb-124 of high specific activity was purchased from ORNL. The chloride solution was converted to a nitrate solution by several treatments with nitric acid followed by evaporation to near dryness. This preparation was added to powdered Nevada glass, melted, redivided, and remelted to ensure homogeneity. The final concentration of the redivided source was roughly 10^{-2} wt-% Sb. As in similar previous experiments,⁽³⁾ an effort was made to obtain a minimum of four points and an order-of-magnitude change in the concentration gradient for each isothermal experiment, and a minimum of four points to define the Arrhenius coefficients for a particular system.

The Nevada matrix used for diffusion measurements with radiocesium⁽²⁾ was finely divided and heated at approximately 1400°C for several days. This was done in an effort to improve the vitreous quality of the matrix, since the first preparation contained a few small bubbles and crystals.⁽²⁾ The glassy character of the silicate was improved by this treatment and, following microscopic examination, a representative sample was analyzed using X-ray diffraction. The diffraction pattern was compared with both the patterns of the original soil sample and the soil that was preheated at 1000°C . Although a few lines were perceptible in the diffraction pattern of the "glass," they were faint and diffuse. The resolution of the camera for this work was roughly 50\AA . The crystallites responsible for the lines could not be ascertained although a search of the ASTM index was made.

Experiments with the diffusion of Sb-124 in the Nevada matrix were done in the temperature range of 1218° to 1766°K . The results are listed in Table 8.

TABLE 8
DIFFUSION COEFFICIENTS FOR THE TRANSPORT OF
RADIOANTIMONY IN THE NEVADA MATRIX

T (°K) ^(a)	D x 10 ⁸ (cm ² /sec) ^(b)
1766	69
1695	32
1599	13
1499	6.0
1416	5.4
1218	3.4

- (a) The uncertainty is approximately 10° K
(b) The uncertainty is approximately 20%

The data from Table 8 are also shown in Fig. 9 where the diffusivity is plotted on a logarithmic scale as a function of the reciprocal temperature. In this figure, it is apparent that the data fall into two sets. Microscopic examination of the samples showed definite signs of devitrification in the low-temperature samples although the high-temperature samples remained glassy. It was concluded that the low-temperature data involved diffusion in increasingly devitrified matrices. The annealing periods for the three low-temperature samples were 16 hr (1218°K), 3 hr (1416°K), and 1.75 hr (1499°K). These times are sufficiently long to allow devitrification if the temperatures are below the liquidus temperature. If this interpretation is correct, then the point of intersection of the two Arrhenius curves in Fig. 9, 1290° C, should correspond to the approximate liquidus temperature of a "representative" glassy Nevada soil. There is some uncertainty associated with the assumption of Arrhenius behavior for the low-temperature data, which are summarized in the following equations:

$$\text{Sb/devitrified Nevada: } \log_{10} D = -6.08 - (1.70 \times 10^3/T). \quad (3)$$

$$\text{Sb/vitreous Nevada: } \log_{10} D = 1.48 - (13.5 \times 10^3/T). \quad (4)$$

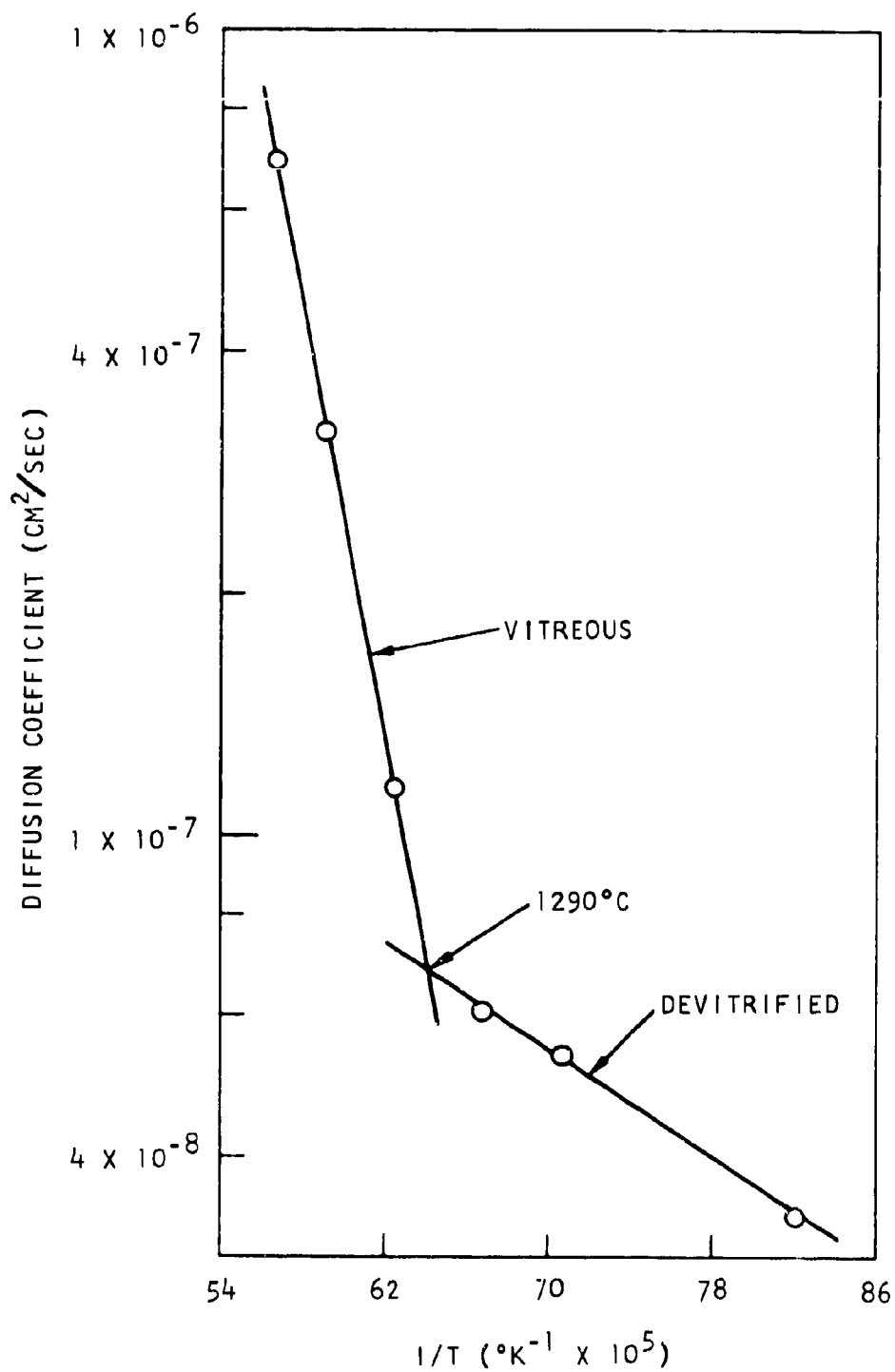


Fig. 9. Diffusion coefficients for transport of Sb-124 in vitreous and devitrified Nevada soil as a function of temperature

Equation (4) is to be compared with the equation for transport of radio-antimony in the 1450°K eutectic of the $\text{CaO-Al}_2\text{O}_3\text{-SiO}_2$ ternary system, (3)

$$\text{Sb/vitreous eutectic: } \log_{10} D = 2.10 - (14.1 \times 10^3/T) . \quad (5)$$

It appears that the transport of Sb in the vitreous Nevada matrix is similar to that in the eutectic matrix. This result strengthens the statement that the $\text{CaO-Al}_2\text{O}_3\text{-SiO}_2$ eutectic matrix is a fair model of vitreous Nevada soil for Small Boy calculations. (2) Note that the times involved in cooling of an atomic-device cloud are small with respect to the time required to complete experiments in the laboratory, and devitrification of a Nevada glass would probably not occur. In this sense, extrapolation of the Arrhenius plot to lower temperatures from the high-temperature data is justified for fallout calculations if the soil has been at sufficiently high temperature. It is anticipated that further diffusion studies will be done using the Nevada matrix.

DIFFUSION IN THE $\text{CaO-Al}_2\text{O}_3\text{-SiO}_2$ SYSTEM

A vaporization technique has been used to study the simultaneous diffusion of several fission-product nuclides in the 1450°K eutectic of the $\text{CaO-Al}_2\text{O}_3\text{-SiO}_2$ system above the liquidus. The results of these studies were reported in a paper submitted for publication in the Advances in Chemistry Series. (8)

The diffusion of several fission-product nuclides in other silicate glasses from this system has been studied in the temperature range of 1508° to 1813°K using the diffusion-couple method. Platinum capillary crucibles were partly filled by melting the matrix in place. The source was then melted in place on top of the matrix. Sources were prepared by dissolving 93% enriched UO_2 in the matrix at the 1% level followed by activation with neutrons using the GGA TRIGA reactor. The sources were allowed to decay somewhat after activation, prior to being used. The capillaries were annealed at 1508°, 1683°, 1773°, and 1813°K for known periods. After annealing, the capillaries were sectioned as in the plane source technique. (3) The capillary length was measured using micrometer calipers after each sectioning, and the abraded material together with the carborundum paper was gamma-analyzed using a Ge-Li detector and a 4096-channel analyzer. With this analyzer, it was possible to monitor many individual fission-product peaks. Often more than one photopeak of a particular species could be studied, thus providing a measure of the internal consistency of the data.

The mathematical model used in these investigations is the solution of the diffusion equation with concentration-independent diffusivity for diffusion from an infinite source into an infinite sink; i. e., the lengths of the source and sink are large with respect to the diffusion distance. The pertinent equation is

$$2C = C_0 \operatorname{erfc} \left(x / 2 (Dt)^{1/2} \right), \quad (6)$$

where C is the concentration of the diffusing species, C_0 is the initial concentration in the source, D is the diffusivity (cm^2/sec) and t is the time. The axis of symmetry of the concentration is at the original interface $x = 0$ of the source and sink where $2C = C_0$. The value of D is obtained by plotting values of C/C_0 against the corresponding values of x on probability graph paper and finding the slope of the best straight line. Experimental data conform well to the model.

Two different matrices were used in these studies. Matrix A wt-% composition was 41 SiO_2 -22 Al_2O_3 -37 CaO , and Matrix B was 52 SiO_2 -18 Al_2O_3 -30 CaO . The experiments using Matrix A were done at 1773°K . These results are listed in Table 9.

TABLE 9
DIFFUSION COEFFICIENTS FOR TRANSPORT OF
FISSION-PRODUCT NUCLIDES IN MATRIX A AT 1773°K

Species	Atomic Mass	$D \times 10^7$ (cm^2/sec)
Te	132	3.5
I	131	3.8
Tc	99	3.5
Zr	95	5.1
Mo	99	3.7
La	140	6.1
Ce	143	4.2

From the data in Table 9, it appears that all of the species diffuse at roughly the same rate with an average diffusivity of $4.2 \times 10^{-7} \text{ cm}^2/\text{sec}$ at 1773°K . Thus, the critical temperature T^* is approximately 1773°K for Matrix A if diffusion for this system is assumed to be compensated. ⁽³⁾

Diffusion in Matrix B was studied at three different temperatures, 1813°, 1683°, and 1508°K. The last temperature is below the liquidus temperature of this ternary composition. It was found that by extrapolating the Arrhenius line, obtained from the two higher temperatures, to 1508°K, most of the experimental diffusivities at this temperature were greatly underestimated. Some devitrification of this matrix probably occurred. The data at 1508°K are not considered pertinent. The data for the two higher temperatures are listed in Table 10.

TABLE 10
DIFFUSION COEFFICIENTS FOR TRANSPORT OF
FISSION-PRODUCT NUCLIDES IN MATRIX B

Species	D x 10 ⁸ (cm ² /sec)	
	1813°K	1683°K
Xe	9.5	2.7
Nd	19	4.9
Ce	19	10
La	30	13
Te	12	3.1
Ba	79	24
Zr	7.5	2.5
Ru	28	4.9

Although the data in Table 10 are preliminary, they afford approximate values of the coefficients in the diffusion equation,

$$\log_{10} D = a - (b/T) \quad (7)$$

The values of a_i and b_i are listed in Table 11.

The data in Table 11 appear to be compensated, i. e., a decreases with b in a fairly regular fashion. In Fig. 10, the compensation correlation is shown for these data. The line drawn through the points is a least-squares-fit to the data with unit weighting assuming a linear correlation. This observation indicates that the results of these preliminary experiments are internally consistent and that compensation prevails for Matrix B. It was also calculated that, on a statistical basis, the "critical" temperature for this system is 1808°K and the "critical" diffusivity is 1.9×10^{-7} cm²/sec.

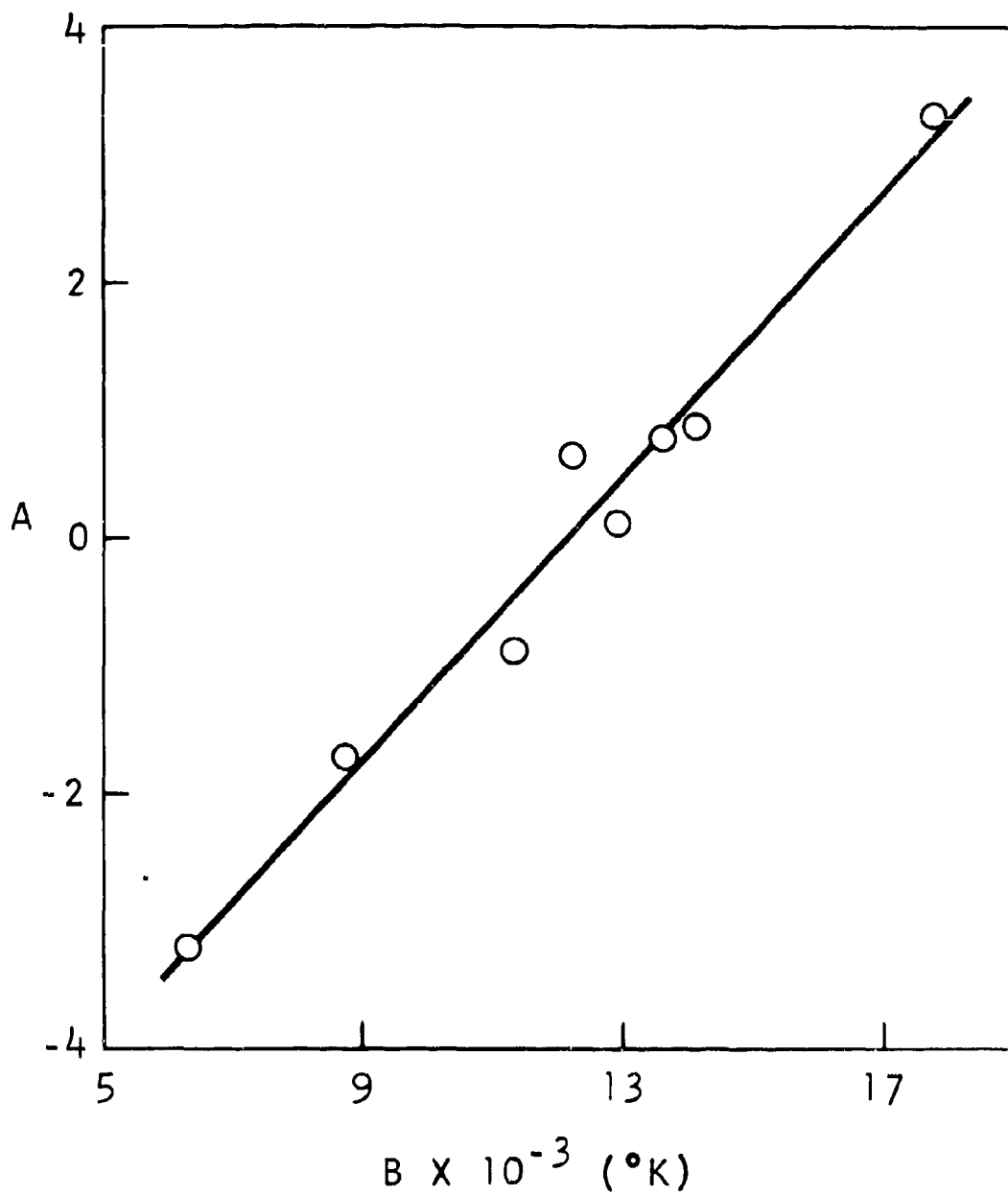


Fig. 10. Compensation correlation for the transport of fission-product species in Matrix B

TABLE 11
COEFFICIENTS IN THE DIFFUSION EQUATION FOR
TRANSPORT IN MATRIX B

Species	a	b x 10 ⁻³ (°K)
Ru	3.29	17.8
Te	0.86	14.1
Nd	0.78	13.6
Xe	0.10	12.9
Ba	0.63	12.2
Zr	-0.90	11.3
La	-1.73	8.7
Ce	-3.23	6.3

Although the results reported here are preliminary, it is possible to compare them with previously reported results(8) for the 1450°K eutectic of the CaO-Al₂O₃-SiO₂ system. In a qualitative sense, diffusion in the eutectic matrix is more rapid than in the more refractory matrices, A and B. A major purpose of this study is to attempt a quantitative evaluation of the effect of composition upon the simultaneous transport of several nuclides in silicate systems. To accomplish this task, more extensive data of this kind are required.

COMPENSATION LAW

The utility of the compensation law, or compensation effect, in predicting the diffusion of fission-product nuclides in silicates has been considered to be important in this laboratory. (2, 3) A paper on this subject has been submitted for publication. (9) The experimental data obtained during this year using the plane-source technique(2) have been combined with previously reported data(2, 3) for diffusion in silicates obtained in this laboratory. The resulting set of 28 datum points has been treated using the compensation effect; the correlation between $\log_{10} D_0$ and $E^*/4.575$, where D_0 is the preexponential coefficient (cm²/sec), and E^* is the activation energy (kcal/mole) in the Arrhenius equation. The correlation is shown in Fig. 11. The curve drawn through the points is the least-squares-fit

$$\log_{10} D_0 = (-4.37 + 0.110 E^*) \pm 0.60, \quad (8)$$

where the uncertainty is the standard error of estimate. The point corresponding to diffusion of radioantimony in the devitrified Nevada matrix

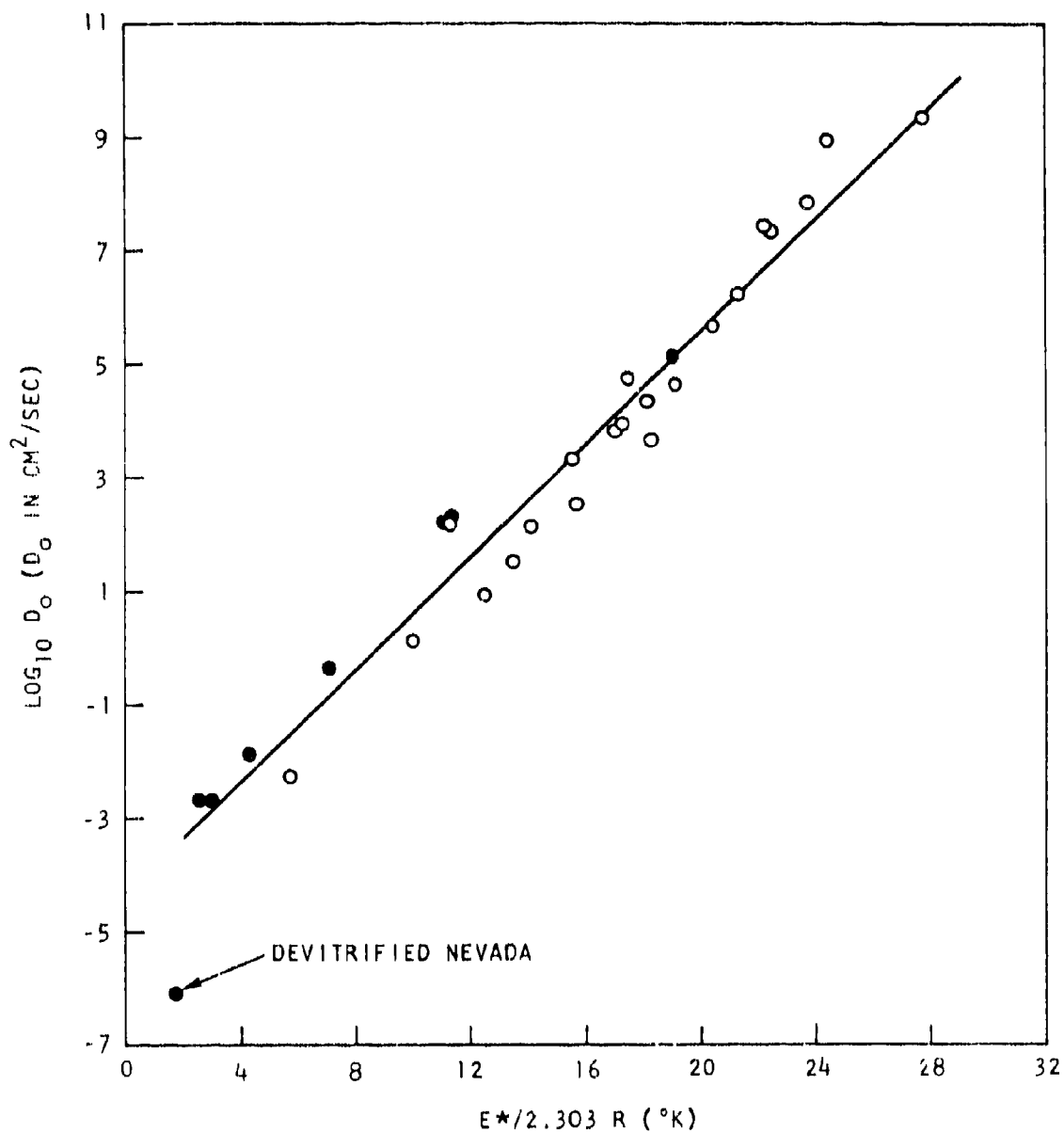


Fig. 11. Compensation correlation for data obtained at GGA for diffusion in silicates. Solid circles refer to data obtained this contract year

was omitted from the least-squares treatment since it is more than four standard deviations from the least-squares line, and transport can certainly be expected to be mechanistically different from that in glasses. The importance of this correlation is that it involves the diffusion of 10 radionuclides in glasses that range in composition from low-refractory sodium disilicate to high-refractory Nevada soil and $\text{CaO-Al}_2\text{O}_3\text{-SiO}_2$. The ranges in the coefficients are roughly 114 kcal/mole for the activation energy and 14 orders of magnitude for D_0 . In a qualitative sense, the correlation can be used to roughly estimate diffusion coefficients since diffusion in refractory matrices and large nuclides involves large values of D_0 and E^* , and diffusion in low-refractory matrices and small nuclides involves small values. Quantitatively, the correlation can be used to predict diffusivities if an independent estimate of either D_0 or E^* can be made. This has been discussed previously. (3) This correlation will be used as the reference for any further calculations done using the Norman⁽²⁾ model and the Korts and Norman⁽¹⁰⁾ calculational scheme.

HENRY'S LAW CONSTANT MEASUREMENTS

In recent reports, ^(2, 11-13) Henry's law data have been presented for several radionuclides in equilibrium with molten matrices from the CaO-Al₂O₃-SiO₂ ternary system. The list of radionuclides that are amenable to experimentation with this system, using the transpiration technique, appears to be exhausted. The two major limitations are satisfactory volatility and lack of interaction with the Pt apparatus. It had been anticipated that a study would be performed using radiotechnetium. However, Tc was found to react with, or diffuse into, Pt and these experiments were discontinued. Further Henry's law constant measurements may be extended to other matrices using fission products already found amenable to study in Pt.

A study was completed that evaluated the effect of gas-phase diffusion on transpiration experiments as done in this laboratory. As a test of the transpiration method used in studying Cs Henry's law constants, ⁽¹³⁾ helium was used in place of Ar carrier-gas. This change was made for both the high- and low-concentration Cs samples described previously. ⁽²⁾ This study was done at approximately 1200°C. Its purpose was to determine if Cs was being transported to the collector in the gas phase. It is possible that, at the lower flow rate, transport limits might have been achieved by diffusion along the walls of the capillary instead of in the gas phase. The reported lack of a complete understanding of the Cs-CaO-Al₂O₃-SiO₂ system, ⁽²⁾ enhanced the importance of this experiment.

Gas-phase diffusivities can be estimated from Hirshfelder's description, ⁽¹⁴⁾

$$D_{1,2} = \frac{0.001858 T^{3/2} [(M_1 + M_2)/M_1 M_2]^{1/2}}{P \sigma_{1,2}^2 \Omega_D}, \quad (9)$$

where $D_{1,2}$ is the interdiffusion coefficient, M is the molecular weight of a gaseous species, $\sigma_{1,2}^2$ is an arithmetic mean cross section, Ω_D is the collision integral evaluated at the geometric mean of kT/ϵ_x (k/ϵ_x is a Leonard-Jones force constant for x), T is the temperature, and P is the pressure. A ratio $D_{1,2}/D_{1,3}$ can be developed,

$$\frac{D_{1,2}}{D_{1,3}} = \frac{\sqrt{\frac{(M_1 + M_2) M_3}{(M_1 + M_3) M_2}}}{\left(\frac{\sigma_1 + \sigma_2}{\sigma_1 + \sigma_3}\right)^2 \left(\frac{\epsilon_3/k}{\epsilon_2/k}\right)^{1/12}}, \quad (10)$$

where $(\epsilon_{1,x}/k)^{1/6}$ is taken as inversely proportional to $\Omega_{D_{1,x}}$, a reasonable assumption for values of $kT/\epsilon_{1,x}$ larger than 10. Above 1200°C this assumption appears to be adequate. Cross sections and values of ϵ_x/k were taken from Hirshfelder, and σ_{Cs} , which is not critical, was taken as 4.5A. The value of $D_{1,2}/D_{1,3}$, where 1 represents Cs-137, 2 represents He, and 3 represents Ar, was calculated to be 2.87. Experimentally comparable $D_{1,x}$ ratios were obtained; 2.2 was obtained for the high Cs concentrations and 2.7 for the low Cs concentrations. These ratios are in excellent agreement with the theoretical value within the experimental error. Thus, gas-phase diffusion is considered to be the controlling process in the Cs transpiration studies at low gas-flow rates.

These new data do not provide an explanation of the lack of oxygen or water-pressure sensitivities described in the last report.⁽²⁾ They do, however, confirm the method of analysis used to describe these previously reported transpiration results.

THE ROLE OF CONDENSATION COEFFICIENTS IN FALLOUT FORMATION

To calculate the importance of condensation coefficients in fallout formation, a system has been developed to evaluate diffusion absorption in spherical particles where a surface reaction plays a role.

Let us assume that the surface condensation rate is proportional to the condensing species pressure P (atm) and reevaporation is proportional to its surface concentration C_s (g/g). Thus, for an isothermal system,

$$\frac{d\bar{C}}{dt} = K\alpha_c P - K'\alpha_e C_s, \quad (11)$$

where \bar{C} is the average concentration of the species in a particle, t is the time (sec), α_c is the condensation coefficient, α_e is the evaporation coefficient, and K and K' are constants. To simplify the system, α_c and α_e will be taken as equal to α , a constant independent of concentration or pressure. At equilibrium

$$0 = \frac{d\bar{C}}{dt} = K\alpha P - K'\alpha C_{sf}, \quad (12)$$

where C_{sf} is the equilibrium surface concentration. Thus, since $P = HC_{sf}$ where H is the Henry's law constant (atm/g/g),

$$KH = K', \quad (13)$$

or

$$\frac{d\bar{C}}{dt} = KH\alpha \left(\frac{P}{H} - C_s \right). \quad (14)$$

For an initial rate of absorption ($C_s = 0$),

$$\left(\frac{d\bar{C}}{dt} \right)_i = K\alpha P, \quad (15)$$

and according to the Langmuir evaporation expression⁽¹⁵⁾

$$\left(\frac{dm}{dt} \right)_i = 44.33 (4\pi r^2) P\alpha \sqrt{M/T}, \quad (16)$$

where m is the quantity condensed (g), r is the radius (cm) of the sphere, M is the molecular weight (g/mole) of the gaseous species, and T is the temperature ($^{\circ}\text{K}$). Now,

$$\left(\frac{dm}{dt}\right)_i = \frac{4\pi r^3 \rho}{3} \left(\frac{d\bar{C}}{dt}\right)_i, \quad (17)$$

where ρ is the particle density (g/cm³) and

$$\left(\frac{d\bar{C}}{dt}\right)_i = \frac{132.99 P \alpha \sqrt{M/T}}{\rho r}, \quad (18)$$

and thus,

$$K = \frac{132.99 \sqrt{M/T}}{\rho r}. \quad (19)$$

It follows, then, that the rate of absorption of a species by the particle is

$$\frac{d\bar{C}}{dt} = \frac{132.99 H \alpha \sqrt{M/T}}{\rho r} \left(\frac{P}{H} - C_s\right). \quad (20)$$

To relate this information to Newman's⁽¹⁶⁾ description of diffusion and surface emission (Crank⁽¹⁷⁾), the term $\frac{d\bar{C}}{dt}$ has to be related to $\frac{dC}{dr}$. Fick's law for a sphere is written

$$\frac{\partial C}{\partial t} = \frac{D}{r_i^2} \frac{\partial}{\partial r_i} \left(r_i^2 \frac{\partial C}{\partial r_i} \right), \quad (21)$$

where D is the diffusion coefficient in the condensed state. Now

$$\begin{aligned} \frac{4\pi r^3}{3} \frac{d\bar{C}}{dt} &= \int_0^r 4\pi r_i^2 \frac{\partial C}{\partial t} dr_i = 4\pi D \int_0^r \frac{\partial}{\partial r_i} \left(r_i^2 \frac{\partial C}{\partial r_i} \right) dr_i \\ &= 4\pi D r^2 \frac{\partial C_s}{\partial r}. \end{aligned} \quad (22)$$

Therefore,

$$\frac{\partial \bar{C}}{\partial t} = \frac{12\pi D r^2}{4\pi r^3} \frac{\partial C_s}{\partial r} = \frac{3D}{r} \frac{\partial C_s}{\partial r} \quad (23)$$

Finally,

$$\frac{\partial C_s}{\partial r} = \frac{44.33 H \alpha \sqrt{M/T}}{D \rho} \left(\frac{P}{H} - C_s \right) = h \left(\frac{P}{H} - C_s \right) \quad (24)$$

as a description of the surface condition where condensation and evaporation coefficients are important. Newnan⁽¹⁶⁾ has solved the diffusion problem for this boundary condition and Crank⁽¹⁷⁾ gives the solution as

$$F = 1 - \sum_{n=1}^{\infty} \frac{6(rh)^2}{\left(\beta_n^2 \left[\beta_n^2 + rh(rh-1) \right] \right)} \exp \left(- \frac{Dt \beta_n^2}{r^2} \right) \quad (25)$$

where F is the fractional absorption where the sphere starts with zero (or uniform) concentration, and

$$\beta_n \cot \beta_n = 1 - rh. \quad (26)$$

The solutions to this problem are presented by Crank for various values of rh . If rh is more than 10 there is little difference between the solution to Eqs. 25 and 26 and that for a strictly diffusion-controlled process. Condensation problems, then, generally become important for rh less than 10. Higher values of rh may become more important at low absorptions. However, as a semiquantitative estimate of the importance of condensation coefficients, if $H = 1$, $T = 1673$, $M = 104$, $\rho = 2.5$, $D = 1 \times 10^{-7}$, and $r = 0.01$, then the α for which condensation problems begin ($rh = 10$) is 2×10^{-6} ; that is, only smaller values of α will cause condensation problems. The values employed were selected from the middle of the ranges of the quantities important for fallout calculations. However, these ranges are wide and, thus, condensation problems are undoubtedly more important than would be suggested by $\alpha_c = 2 \times 10^{-6}$ limit. Adams⁽¹⁸⁾ has used values of α this low and lower to explain some experimental data.

In a more exact application of Eqs. 25 and 26 to the problem of fallout, difficulty in calculation at low absorptions is encountered. For fallout

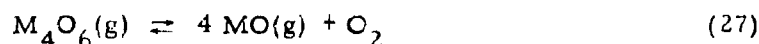
problems, important values of F are often below 0.1. This involves values of n , r , D , t , and β_n such that the series in Eq. 25 is slowly converging. Attempts were made to transform this equation or to simplify it to render calculation simpler. First attempts have been unsuccessful. It appears that a computer program is required to accurately evaluate this question throughout the entire range of F values.

Another planned test of this system is the use of the SLIDER Code,⁽⁸⁾ described at the April 1968 symposium on fallout, to calculate the effects of combinations of gas-phase diffusion, condensed-state diffusion, and condensation rate on absorption by a spherical particle. Numerical calculations of this kind should be useful in describing recent work by Adams⁽¹⁸⁾.

MASS SPECTROMETRY OF OXIDE SYSTEMS

The molecular character of gaseous-fission products and their oxides is of critical importance in describing fallout formation. These considerations are involved in many of the mechanisms of particle-gas interaction; e. g., gas-phase diffusion, condensation, Henry's law equilibria, condensed-state diffusion, and reevaporation. During the past year, the method of high-temperature Knudsen-cell mass spectrometry has been used to define gaseous equilibria between metals, metallic oxides, and O for Sb, As, and Te.

An attempt to evaluate the stabilities of MO(g) and $\text{MO}_2\text{(g)}$ ($\text{M} = \text{As, Sb}$) has been made. In particular, the reaction



was studied. The metal oxides were dissolved in B_2O_3 to reduce their activities. These melts were placed in an Ir Knudsen cell provided with an oxygen inlet. The cell was heated by radiation and electron bombardment. Temperatures were measured by either a Pt-Pt 10% Rh thermocouple or an optical pyrometer. The molecules $\text{M}_4\text{O}_6\text{(g)}$, MO(g) and O_2 were the only species observed effusing from the Knudsen cell under these conditions. Appearance potentials of the oxides were found to be 10.6, 8.9, 9.9, and 9.0 eV for As_4O_6^+ , AsO^+ , Sb_4O_6^+ , and SbO^+ , respectively, with an estimated uncertainty of 0.5 eV.

Isothermal dependence of the peak intensity ratio $\text{M}_4\text{O}_6^+:(\text{MO}^+)^4$ on the O_2^+ signal showed that Reaction 27 was being studied.

Temperature-dependence measurements of the equilibrium constants for Reaction 27 were made. Four determinations were made for each reaction with an average of 7 points each. Figure 12 and 13 are typical temperature-dependence plots for Reaction 27 for As and Sb.

Entropies for this reaction were calculated from equilibrium constants obtained from Ag pressure calibrations of the systems. Table 12 is a summary of the heats and entropies. The data, including the lack of observation of $\text{MO}_2\text{(g)}$, suggest that MO(g) may be the important gaseous species for these elements during fallout formation.

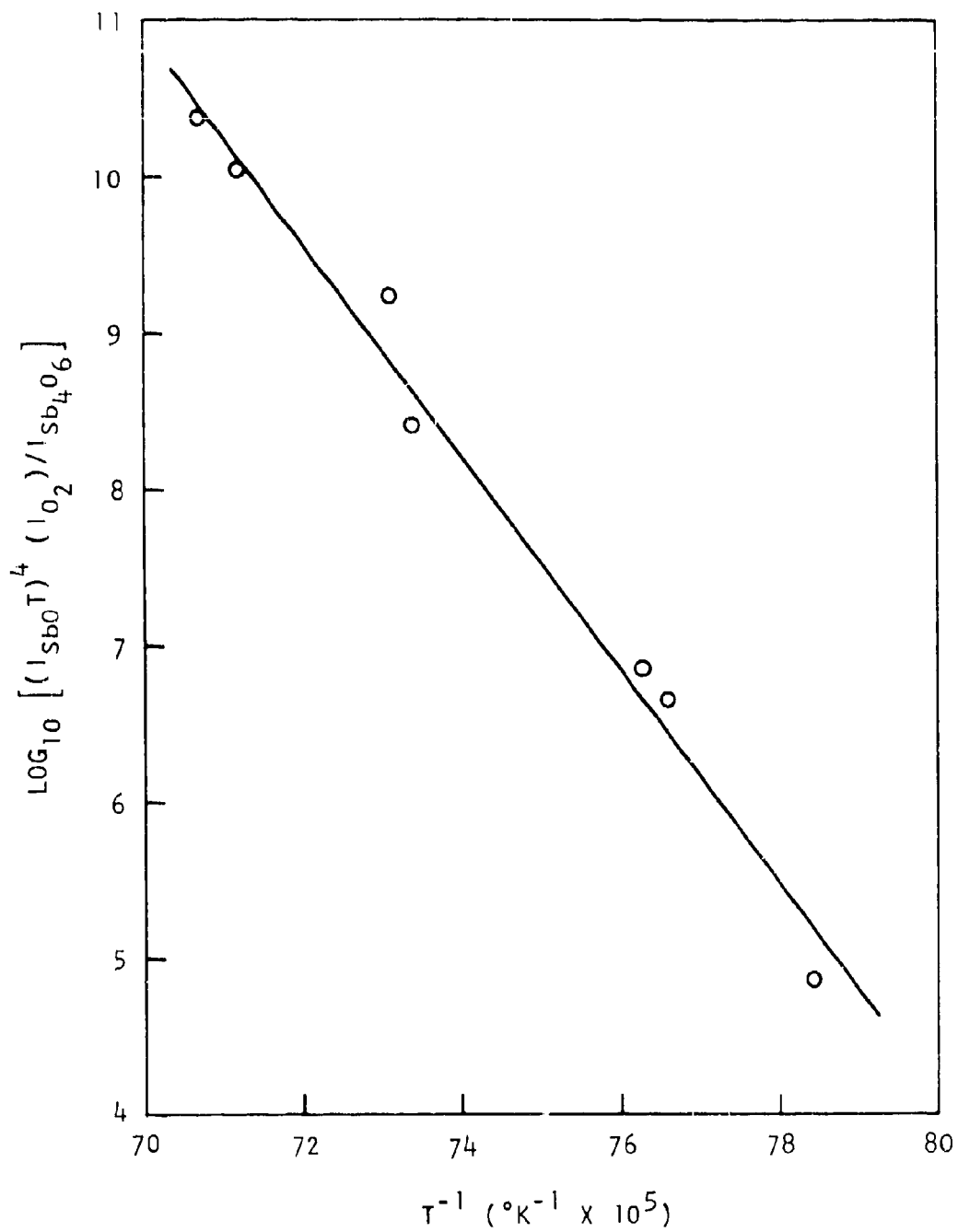


Fig. 12. A typical temperature dependence of the equilibrium constant of Reaction 27 for As

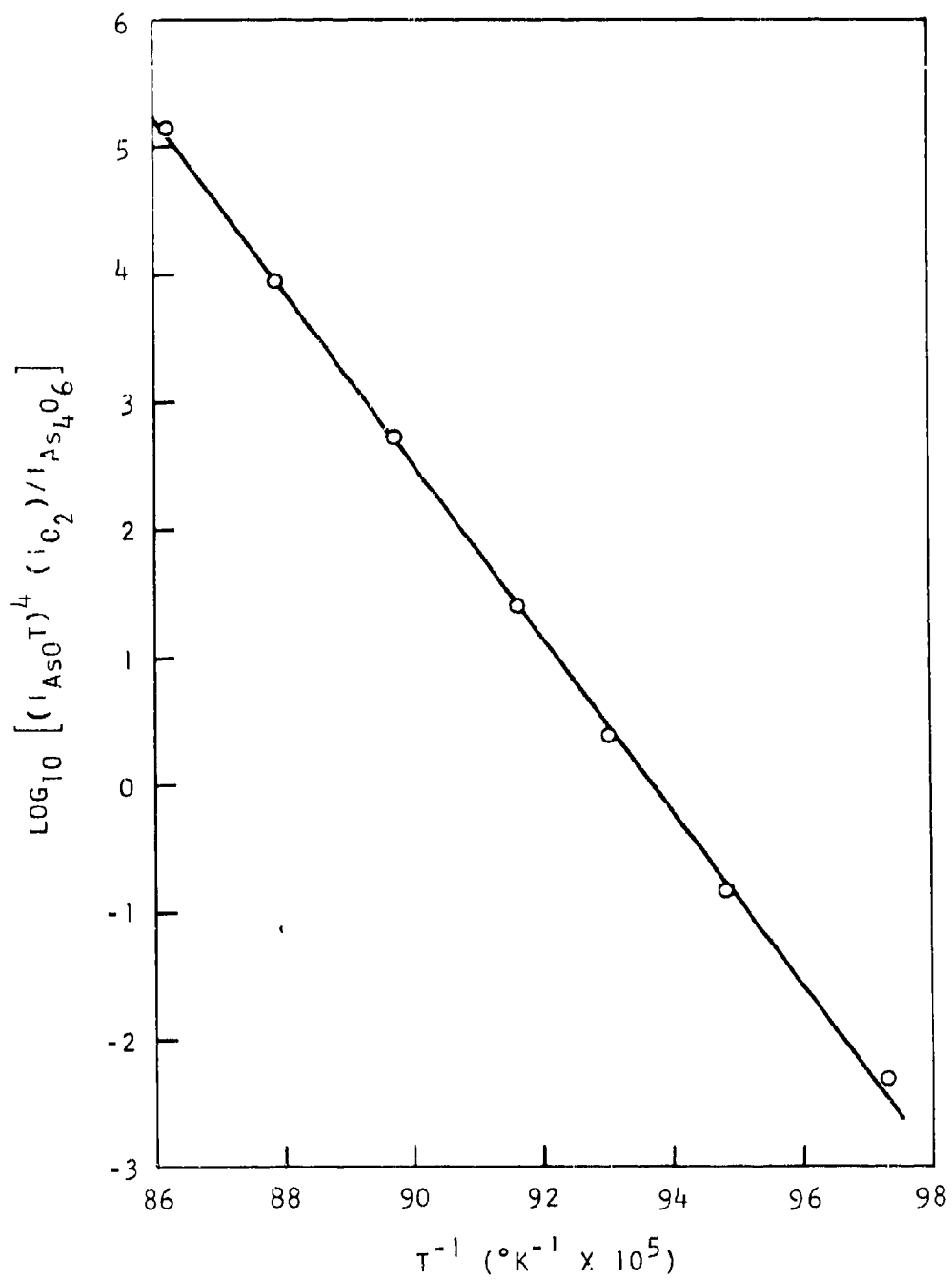


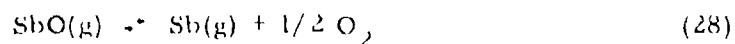
Fig. 13. A typical temperature dependence of the equilibrium constant of Reaction 27 for Sb

TABLE 12

SUMMARY OF THE HEATS AND ENTROPIES FOR REACTION 27

M	Temp. Range (°K)	$\Delta H_{\text{mid-temp}}$ (kcal/mole)	$\Delta S_{\text{mid-temp}}$ (eu)
As	1025 - 1175	309 ± 4	147
Sb	1285 - 1415	315 ± 6	128

A study of the reaction



has also been completed.

A mixture of Na_2CO_3 and Sb_2O_3 , which had been heated to its melting point, was put into an Ir Knudsen cell. The cell was placed in the mass spectrometer and heated by electron bombardment. Temperatures were measured with an optical pyrometer.

The ions O_2^+ , Sb^+ , and SbO^+ were observed after considerable CO_2 was evolved. Appearance potentials were found to be 8.7 and 8.1 eV for Sb^+ and SbO^+ , respectively. The appearance potential for Sb^+ is in good agreement with 8.6 eV reported in Kiser's compilation.⁽¹⁹⁾ The appearance potential for SbO^+ is 0.9 eV lower than that found during the study of Reaction 27. The value of 8.1 eV is believed to be more reliable because the SbO^+ signal was a factor of 50 higher.

Four sets of temperature-dependence measurements of the equilibrium constant for Reaction 28 were made. They yielded a $\Delta H^\circ_{1493} = 38.1 \pm 1.6$ kcal/mole. The temperature range of the measurements was 1405° to 1582°K. A silver calibration was done and partial pressures were calculated. An entropy was calculated for Reaction 28 from the equilibrium constant obtained from the pressure calibration. Table 13 is a summary of the results.

A ΔH°_{1500} of 467 kcal/mole is obtained for

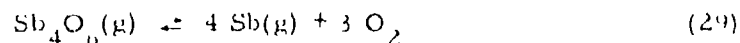


TABLE 13

RESULTS OF THE PRESSURE CALIBRATION AND
CALCULATED ENTROPY FOR REACTION 28

Temp (°K)	P _{SbO} (atm)	P _{Sb} (atm)	P _{O₂} (atm)	ΔS (eu)
1496	1.13×10^{-6}	5.63×10^{-6}	2.38×10^{-6}	11.2

by combining the results of Reactions 27 and 28. Using ΔH_{1500}^0 60.7 kcal/mol⁽²⁰⁾ for $1/2 O_2 \rightleftharpoons O$ and 315 kcal/mole for Reaction 27 as reported previously, values of 98.8 kcal/mole for SbO(g) and 831 kcal/mole for Sb₄O₆(g) are obtained for D_{1500}^0 .

Gaydon⁽²¹⁾ reports a dissociation energy, D_G^0 of 74 ± 9 kcal/mole at 0°K for SbO(g). This value is an extrapolated spectroscopic value in which the ground state of the molecule was uncertain. Brewer⁽²²⁾ reports an energy of dissociation to the atoms at 0°K for Sb₄O₆(g) of 886 ± 15 kcal/mole, a difference of only 4% from the value found in this study.

The Te-O system is described elsewhere.⁽²³⁾

PUBLICATIONS AND PRESENTATIONS

The papers listed below describe investigations that were completely or partly supported by contracts with the Office of Civil Defense, Office of the Secretary of the Army, and Department of Defense through the U. S. Naval Radiological Defense Laboratory, and have been presented, submitted, or published during the past year. They should be regarded as part of the final report.

J. H. Norman, P. Winchell, J. M. Dixon, B. W. Roos, and R. F. Korts, "Spheres: Diffusion-Controlled Fission Product Release and Absorption," presented at the American Chemical Society National Meeting, San Francisco, 1968; submitted for publication in Advances in Chemistry Series.

J. H. Norman, P. Winchell, H. G. Staley, M. Tagami, and M. Hiatt, "Henry's Law Constant Measurements for Fission Products Absorbed in Silicates," in Thermodynamics of Nuclear Materials, 1967, IAEA, Vienna, 1968, p. 209.

H. G. Staley, "A Mass-Spectrometric Knudsen-Cell Study of the Gaseous Oxides of Tellurium," submitted for publication in the Journal of Chemical Physics, October 31, 1968.

P. Winchell, "The Compensation Law for Diffusion in Silicates," to be published in the Journal of High Temperature Science, September 27, 1968.

H. G. Staley and J. H. Norman, "Thermodynamics of Reactions Between the Monoxides and Dioxides of Ce, Pr and Nd," Int. J. Mass Spect. Ion Phys. 2, 35 (1969).

REFERENCES

1. Gordon, G. E., J. W. Harvey, and H. Nakahara, Nucleonics **24**, 62 (1966).
2. Norman, J. H., P. Winchell, and H. G. Staley, "Cloud Chemistry of Fallout Formation: Final Report," U. S. Naval Radiological Defense Laboratory Report GA-8472, Gulf General Atomic Incorporated, 1968.
3. Winchell, P., and J. H. Norman, "A Study of the Diffusion of Radioactive Nuclides in Molten Silicates at High Temperatures," Third International Symposium on High-Temperature Technology Proceedings, September 17 through 20, 1967, at Asilomar, California, to be published.
4. Lane, W. B., "Fallout Simulant Development: Temperature Effects on the Sorption Reactions of Cesium on Feldspar, Clay and Quartz," Stanford Research Institute, Project No. MU-6014, 1967.
5. Schairer, J. F., and N. L. Bowen, Am. J. Sci. **254**, 162 (1956).
6. Malkin, V. I., and B. M. Mogutnov, "Measurement of Coefficients of Cation Self-Diffusion in Silicate Melts by Means of Radioisotopes Na^{24} , K^{42} and Ca^{45} ," in Radioisotopes in the Physical Sciences and Industry, Vol. I, IAEA, Vienna, 1962 (p. 169).
7. Dertev, N. K., and Z. P. Voronkova, "Electrochemical Method for Determining Diffusion Coefficients of Silicate Melts," in The Structure of Glass 4, Electrical Properties and Structure of Glass, O. V. Mazurin (ed.) Consultants Bureau, New York, 1965.
8. Norman, J. H., et al., "Spheres: Diffusion-Controlled Fission Product Release and Absorption," presented at American Chemical Society National Meeting, San Francisco, March-April 1968; to be published in the Advances in Chemistry Series.
9. Winchell, P., "The Compensation Law for Diffusion in Silicates," to be published in the Journal of High Temperature Science.

10. Korts, R. F., and J. H. Norman, "A Calculational Model for Condensed State Diffusion Controlled Fission Product Absorption During Fallout Formation," U. S. Naval Radiological Defense Laboratory Report GA-7598, General Dynamics, General Atomic Division, 1967.
11. Norman, J. H., et al., "Henry's Law Constant Measurements for Fission Products Absorbed in Silicates," in Thermodynamics of Nuclear Materials 1967, IAEA, Vienna, 1968, p. 209.
12. Norman, J. H., and P. Winchell, "Cloud Chemistry of Fallout Formation," "Part I. Fallout Phenomena Symposium Proceedings," U. S. Naval Radiological Defense Laboratory Reports USNRDL-R and L-177, 1966.
13. Norman, J. H., and P. Winchell, "Cloud Chemistry of Fallout Formation: Final Report," U. S. Naval Radiological Defense Laboratory Report GA-7597, Gulf General Atomic Incorporated, 1967.
14. Hirshfelder, J. O., C. F. Curtiss, and R. B. Bird, Molecular Theory of Gases and Liquids. John Wiley and Sons, Inc., New York, 1954.
15. Gilles, P. W., "Vaporization Processes" in The Characterization of High Temperature Vapors, J. L. Margrave, (ed.) John Wiley and Sons, Inc., New York, 1967, p. 33.
16. Newman, A. B., Trans. Am. Inst. Chem. Engrs. 27, 203 (1931).
17. Crank, J., The Mathematics of Diffusion, Clarendon Press, Oxford, 1956, p. 91.
18. Adams, C. E., W. R. Balkwell, and J. T. Quan, "High Temperature Measurements of the Rates of Uptake of Molybdenum, Tellurium and Rubidium Oxide Vapors by Selected Oxides," 155th National American Chemical Society Meeting, San Francisco, March 31-April 5, 1968.
19. Kiser, R. W., OTS-U.S. Dept. of Commerce, TID-6142, 1960.
20. Stull, D. R., and G. C. Sinke, Thermodynamic Properties of the Elements, American Chemical Society, Washington, D. C., 1956, p. 144.

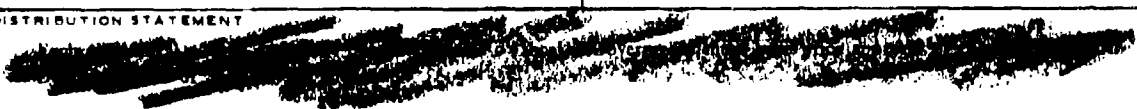
21. Gaydon, A. G., Dissociation Energies and Spectra of Diatomic Molecules, Chapman and Hall, Ltd., London, 1953, p. 231.
22. Brewer, L., Chem. Rev. 52, 47 (1953).
23. Staley, H. G., "A Mass-Spectrometric Knudsen Cell Study of the Gaseous Oxides of Tellurium," to be published in the Journal of Chemical Physics.

UNCLASSIFIED

Security Classification

DOCUMENT CONTROL DATA - R & D

Security Classification of title, body of abstract and indexing annotation must be entered when the overall report is classified

1. ORIGINATOR'S NAME (Corporate author)		2a. REPORT SECURITY CLASSIFICATION	
Gulf General Atomic Incorporated San Diego, California		Unclassified	
3. REPORT TITLE		2b. GROUP	
Cloud Chemistry of Fallout Formation Final Report			
4. DESCRIPTIVE NOTES (Type of report and inclusive dates)			
5. AUTHOR(S) (First name, middle initial, last name)			
John H. Norman, Perrin Winchell, and Harry G. Staley			
6. REPORT DATE	7a. TOTAL NO. OF PAGES	7b. NO. OF REFS	
January 31, 1969	64	23	
8a. CONTRACT OR GRANT NO	9a. ORIGINATOR'S REPORT NUMBER(S)		
N0022868C2376	GA-9180		
a. PROJECT NO	9b. OTHER REPORT NO(S) (Any other numbers that may be assigned this report)		
c.			
d.			
10. DISTRIBUTION STATEMENT			
			
11. SUPPLEMENTARY NOTES		12. SPONSORING MILITARY ACTIVITY	
		Office of the Civil Defense Office of the Secretary of the Army Washington, D.C., 20301	
13. ABSTRACT			
<p>Studies of fission-product gamma emanation shortly after fission (1 to 100 sec) have been initiated. The half-lives that will be established in this program, when used in conjunction with initial yields, will provide the fission-product yield history for calculational models. The studies undertaken include (1) an investigation of the transitive behavior of fission products from approximately 1 sec after fission, (2) experiments to establish recoil range as a parameter to use for identifying the sources of specific gamma rays, and (3) design of a steady-state tape system for catching and subsequently investigating recoil-fission products. This latter study is the result of earlier investigations and shows promise of providing extensive, accurate data on fission-product half-lives.</p> <p>Studies of diffusion of various nuclides in the $\text{CaO-Al}_2\text{O}_3\text{-SiO}_2$ system, the $\text{Na}_2\text{O-Al}_2\text{O}_3\text{-SiO}_2$ system, and Small Boy soil from the Nevada test site have been made. The use of fission products from slow U-235 fission in situ has been demonstrated as a surveying method for studying diffusion in various matrices doped with U-235. The results of the studies are consistent with the compensation law, particularly with the compensated data developed previously in this program. The liquid-structure factor appears to be important in establishing diffusivities.</p> <p>Transpiration studies of the volatility of Cs from $\text{CaO-Al}_2\text{O}_3\text{-SiO}_2$ solutions indicate that simple gas-phase transport laws apply to transpired Cs. The condensed-state and vapor-state chemistry of this system have not been totally resolved.</p> <p>A mathematical description of sorption of gaseous components by a particle, using condensation coefficients and condensed-state diffusion coefficients, is presented. This treatment suggests that condensation coefficients become important to the process only when they are lower than approximately 2×10^{-6}.</p> <p>Mass spectrometric studies have been made that provide estimates of the stabilities of the gaseous species Sb_4O_6, As_4O_6, SbO, TeO, and TeO_2. The gaseous species AsO_2 and SbO_2 were not observed, thus their stabilities could not be measured.</p>			

DD FORM 1473

1 NOV 68

UNCLASSIFIED

Security Classification

14 KEY WORDS	LINK A		LINK B		LINK C	
	ROLE	WT	ROLE	WT	ROLE	WT
Fission-product fractionation Henry's law constant Fission-product absorption Diffusion studies Fallout formation Cloud chemistry High-temperature chemistry Mass spectrometry Transpiration studies Short-lived fission products Radioactive half-life studies Fission recoil-range studies Gamma-ray spectrum Molten silicates Compensation law Small Boy soil Condensation coefficient Knudsen-Cell studies						